Review

3D Cell Printed Tissue Analogues: A New Platform for Theranostics

Yeong-Jin Choi[1]*, Hee-Gyeong Yi[2]*, Seok-Won Kim[2] and Dong-Woo Cho[2]✉

1. Division of Integrative Biosciences and Biotechnology, Pohang University of Science and Technology (POSTECH), 77 Cheongam-ro, Nam-gu, Pohang, Gyeongbuk 790-781, Republic of Korea;
2. Department of Mechanical Engineering, Pohang University of Science and Technology (POSTECH), 77 Cheongam-ro, Nam-gu, Pohang, Gyeongbuk 790-781, Republic of Korea.

* These authors contributed equally to this work.

✉ Corresponding author: Professor Dong-Woo Cho, Department of Mechanical Engineering, Pohang University of Science and Technology, 77 Cheongam-ro, Nam-gu, Pohang, Gyeongbuk 790-784, Korea. Tel: +82-54-279-2171; Fax: +82-54-279-5419. E-mail address: dwcho@postech.ac.kr.

Abstract

Stem cell theranostics has received much attention for noninvasively monitoring and tracing transplanted therapeutic stem cells through imaging agents and imaging modalities. Despite the excellent regenerative capability of stem cells, their efficacy has been limited due to low cellular retention, low survival rate, and low engraftment after implantation. Three-dimensional (3D) cell printing provides stem cells with the similar architecture and microenvironment of the native tissue and facilitates the generation of a 3D tissue-like construct that exhibits remarkable regenerative capacity and functionality as well as enhanced cell viability. Thus, 3D cell printing can overcome the current concerns of stem cell therapy by delivering the 3D construct to the damaged site. Despite the advantages of 3D cell printing, the *in vivo* and *in vitro* tracking and monitoring of the performance of 3D cell printed tissue in a noninvasive and real-time manner have not been thoroughly studied. In this review, we explore the recent progress in 3D cell technology and its applications. Finally, we investigate their potential limitations and suggest future perspectives on 3D cell printing and stem cell theranostics.

Key words: Three-dimensional (3D) cell printing, stem cell theranostics

Introduction

Stem cell therapy holds great promise for the treatment of diseases and injuries because implanted stem cells can directly differentiate into target cells or secrete therapeutic paracrine molecules to the lesion site [1, 2]. Along with the great attention that has been given to stem cell therapy, stem cell theranostics, which tracks and monitors the delivered cells in a noninvasive manner by using imaging agents and imaging modalities, is a promising technique for improving the understanding of the implanted cells' dynamics, including their viability, differentiation, migration, and engraftment *in vivo* [3, 4]. However, the limited efficacy of stem cell therapy, including

unpredictable cell destination, low cellular retention, low survival rate, and low engraftment after transplantation, has been a major concern. Although tissue-engineered scaffolds have been considered as a carrier for stem cell therapy, they could not replicate tissue complexity, so stem cells may lose their regenerative potency [5-7]. Three-dimensional (3D) cell printing is an emerging technology in the field of regenerative medicine. 3D cell printing enables a 3D complex living tissue to be built with precise spatial control for the placement of biomaterials, biomolecules, and cells [8]. This technology facilitates the generation of the patient's specific tissue

constructs by using computer-aided design (CAD) and computer-aided manufacturing (CAM), which can design and process the complex architectural tissue information collected from medical imaging technologies, such as computed tomography (CT) and magnetic resonance imaging (MRI) [9, 10]. Bioinks refer to cell-encapsulating biomaterials (usually hydrogels) that allow the printed mass to be constructed into a 3D form, as well as provide a cell matrix to substitute or mimic native tissue [6, 11, 12]. Therefore, a suitable microenvironment providing physical, chemical, and biological cues for accelerating the tissue formation can be controlled by the selection of bioinks [7]. To date, complete organs or tissues that recapitulate tissue complexity, vascularization, and innervation have not been printed, but some of the features and functions of cell printed constructs have nearly reached the level of native tissue [13]. Although current 3D cell printing approaches are still in the early stages, cell printed constructs have been considered as potentially transplantable tissues, including bone, cartilage, muscle, and skin, due to their remarkable regeneration capacity [14-18]. Recently, 3D cell printing has not only been utilized to build the 3D tissue construct for the purpose of tissue repair or regeneration, but also as a powerful tool for drug testing and discovery, by fabricating a 3D *in vitro* model that reflects the pathological environment of the patient. [19]. Therefore, 3D cell printing can enhance the regenerative efficacy of stem cell therapy and deliver the stem cells to the lesion site while maintaining their functionality and viability [20]. However, it is still not clear how the cells attach, grow, and differentiate in the 3D construct and dynamically interact with the host tissue during the tissue regeneration process. In this regard, appropriate technologies are necessary to monitor and assess the cellular behavior as well as the regenerative capacity of a 3D cell printed tissue in a noninvasive and simultaneous manner. Recent cell (or stem cell) labeling and tracking techniques are able to noninvasively monitor and trace the implanted cells as well as cellular activity, such as viability, differentiation, and migration, with high spatial resolution for long periods [21]. Thus, integrating the stem cell-tracking technique and 3D cell printing would possibly generate a synergistic effect in the field of regenerative medicine. In this review, we introduce the latest advances in 3D cell printing technology and its applications. Finally, we discuss the current challenges of 3D cell printing and suggest a future paradigm for a new theranostics strategy using 3D cell printing technology.

Recent advances in 3D cell printing technology

Printing technologies

3D printing has emerged as a novel manufacturing technology since Hull introduced stereolithography (SLA, 3D Systems, CA, USA) in 1986 [22] and is growing as a revolutionary alternative to conventional methods (e.g., molding, milling, and turning) in diverse areas, including biomedical tools, tissue engineering, organs-on-chips, and microfluidic devices. Although numerous techniques that are adaptable to 3D printing have been reviewed in the literature [19, 20, 23], here we describe some representative working principles of 3D cell printing and its materials for potential applications in tissue engineering.

Laser-based printing

SLA is the oldest technique that allows for the production of an arbitrary shape in an assembly-free manner by focusing a light source on a spot in a photo-sensitive liquid following a pre-defined path to form a 3D volumetric structure (**Figure 1a**). The resolution is determined by the laser spot size and absorption wavelength range of the photoresins. Two-photon laser-scanning SLA has been used to precisely fabricate small features in the microscale, such as a substrate with an extracellular matrix (ECM)-mimicking topology with a diameter of ~100 nm [24], 115-μm-high ultracompact multi-lens objectives [25], and multiple arrays of microneedles with a diameter of 150 μm for transdermal drug delivery [26]. Digital light projection (DLP) SLA enables the photo-polymerization process to be accelerated by exposing an entire layer of photosensitive materials to a projected beam at once, and the resolution depends on the pixel size. Owing to the reduction in the price of digital micromirror display technology, DLP printers are less expensive than other SLA printers [27]. SLA printers are also capable of building a 3D cell-laden microstructure by irradiating the hydrogel containing both cells and the UV-sensitive cross-linkers [28, 29].

Laser-assisted printing offers the direct deposition of materials on a free surface based on the "aim-and-shoot" procedure, while SLA builds a construct dipped in a photocurable liquid, resulting in an additional process for removing the uncured materials. A laser-assisted printing system typically consists of a laser-absorbing layer, called the ribbon, a feeding layer of cell-laden hydrogel beneath, and a receiving substrate (**Figure 1b**). When the laser pulse is focused on the laser-absorbing layer (the "aim" step), a vapor pocket is generated in the feeding layer,

resulting in the falling off of the cell-laden droplet (the "shoot" step) to the receiving substrate [19]. This technology offers a high resolution (~40-µm droplet diameter [30]) owing to the accuracy of laser targeting itself. The resolution is determined by the laser source, the thickness of the feeding layer, and the gap distance from the ribbon to the receiving substrate. Additionally, although it is still challenging to photo-polymerize multiple materials for fabricating a heterogeneous structure with SLA, it is feasible to build a construct with multiple materials by sequentially changing the feeding layers with laser-assisted printing [31].

Inkjet-based printing

The printing of living tissue began from the 2D patterning of cells with a modified version of commercialized inkjet printers, such as the Hewlett-Packard Desktop printer (HP550C; Hewlett-Packard Company, CA, USA) and its cartridge [32]. The inkjet cartridge generates cell-laden drops and ejects them onto a substrate, called bio-paper, in a "drop-on-demand" fashion. The drops can be separated from a continuous flow of bioink passing through the nozzle by generating a bubble in the flow. The bubble is usually produced by local heating of the nozzle or by physical breaking using a piezoelectric actuator (**Figure 1c**). The heating method instantaneously increases the temperature to evaporate the ink, making the bubble and the ink droplet. On the other hand, a piezoelectric actuator physically breaks the ink and is therefore preferred for application in cell printing [19]. Although the viscosity of cell-laden hydrogel is restricted to around 0.1 Pa·s [33], this printing method offers high-resolution droplet printing (~20 µm [34]) and is promising for narrowing down the scale of complex biological structures.

To construct a 3D shape by stacking the ejected droplets, the multi-jet modeling method has been developed by incorporating photo-polymerization into inkjet printing systems. The configuration is composed of inkjet heads, a UV irradiator, and a building platform with an elevator (**Figure 1d**). The inkjet heads deliver photopolymers onto the tray, and the UV lamp is moved directly above the ejected droplet for rapid polymerization. Likewise, this printing method provides rapid multiple materials construction, including transparent polymers, an uncured material-free process, and high resolution (~300-µm gap distance), and it has become an attractive technology for fabricating small cell-culturing devices, such as microfluidic channels and chips [27].
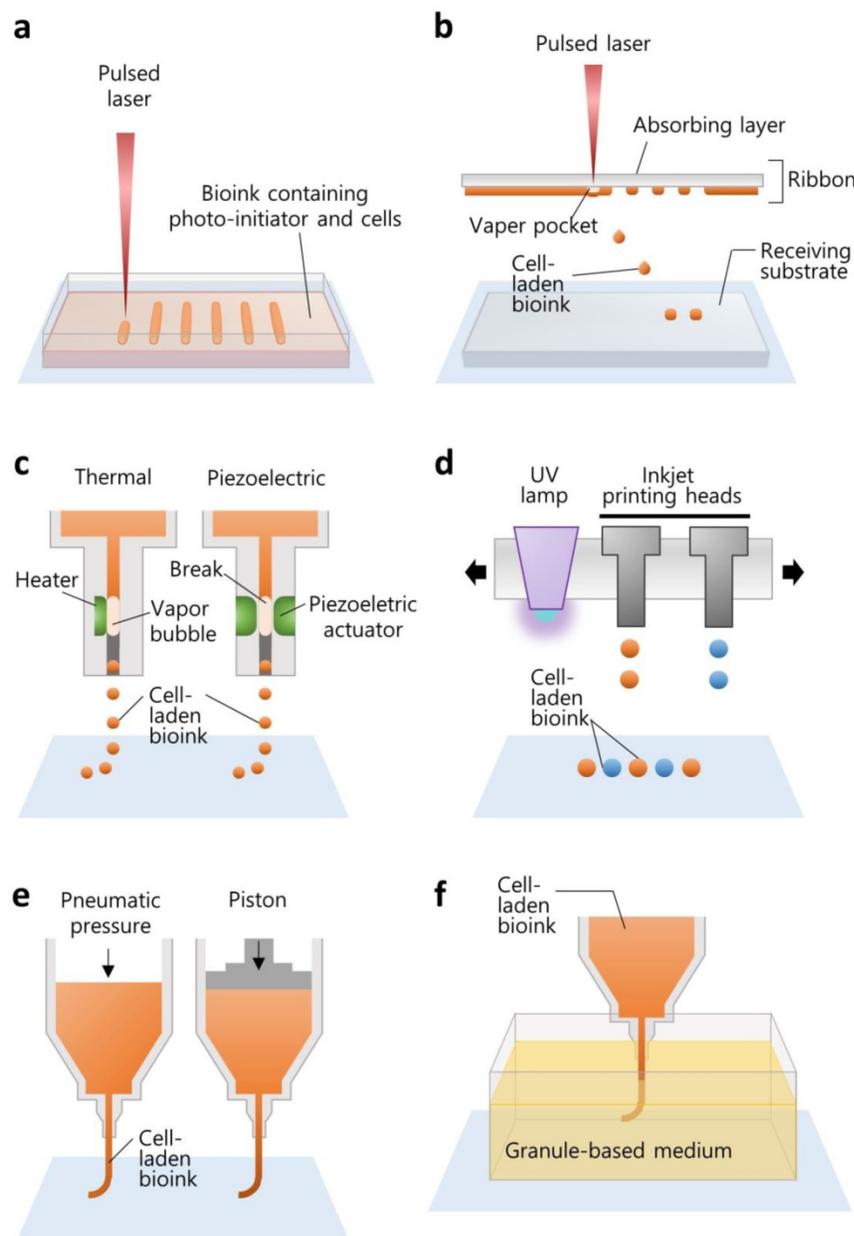

Figure 1. Illustrations elucidating the various working principles of 3D printing techniques for building biological constructs. The techniques include (a) SLA, (b) laser-assisted printing, (c) inkjet printing, (d) multi-jet modeling, (e) extrusion printing, and (f) granule-based medium-assisted printing.

Extrusion-based printing

After Crump invented fused

deposition modeling (FDM, Stratasys, MN, USA), which extrudes a molten thermoplastic filament through a nozzle by motor-driven force, extrusion printing systems became a common strategy in diverse areas. Extrusion printing has been widely used to fabricate implantable scaffolds for tissue regeneration [35] and drug-releasing biodegradable constructs for local drug delivery [36, 37]. For printing cells or gel-forming materials, extrusion printing systems typically move a syringe containing the materials in 3D space and dispense a continuous stream by piston-driven or pneumatic forces (**Figure 1e**) [38]. Hence, this method enables printing higher concentrations of hydrogels (≥0.03 Pa·s [20]) and brings unique benefits when printing large volume cell-laden constructs [10]. Although a SLA printer can move the laser focus faster than the printing head moves in extrusion-based printing, the selection of bioink is limited to a photopolymerizable material [39]. Inkjet-based printing can jet 1–10000 droplets/s [20], but the thickness of the printed strut is also limited due to the low concentration of hydrogel [10]. In this sense, extrusion-based printing is advantageous for the fast generation of large constructs. Moreover, this printing method offers not only various options for selecting building materials, including thermoplastic polymers, hydrogels, and cells, but also combinatorial construction by simply alternating the printing heads containing different materials. For instance, our group developed an in-house extrusion printing system with multiple heads and have demonstrated the co-printing of heterogeneous living tissues for tissue engineering and organ-on-chip applications [10, 40-42].

Although the external pushing forces allow the use of materials with a wide range of viscosities [20], it is not easy to achieve high shape fidelity and printability with hydrogel printing while maintaining a suitable cellular environment. The *biofabrication window* is a concept that describes the compromise between the physical and biological properties of a bioink [43]. High biofunctionality including cell viability, proliferation, migration, and differentiation is typically achieved with soft hydrogels. However, due to the inherently weak strength and low printability of the soft hydrogels, they cannot generate a fine construct that maintains a 3D structure for continued cellular function. In contrast, a bioink that has high printability is generally attained by increasing the hydrogel concentration or increasing cross-linking density, which hinders biofunctionality. Hinton *et al*. proposed a method for the reversible embedding of a dispensed hydrogel within a granule-based medium (**Figure 1f**) [44]. They

developed a gelatin slurry support bath to maintain the shape of the printed alginate precursor during its complete gelation. After removing the liquid support, they demonstrated the construction of a complex biomimetic structure. Similarly, the printing of a soft material with a complex design was also achieved by embedding polydimethylsiloxane (PDMS) elastomer into a hydrophilic support bath composed of Carbopol® [45]. This support bath-based printing technique facilitates the deposition of bioinks and the fabrication of a 3D fine construct even if the bioink has low printability and a low cross-linking density. This printing technique can overcome the drawbacks associated with the weak printability of bioink while maintaining adequate biofunctionality.

Bioinks for printing cells

Bioink is a cell-suspended, viscoelastic solution that protects the cells from exogenous stress and other dangerous factors arising from the printing process by encapsulating the cells within it. Additionally, bioinks usually form a matrix for cell growth. Here, we discuss the assorted hydrogels currently used as bioinks. In addition, we summarize the bioinks used in 3D cell printing, including their cell viability, their target tissue to regenerate, their cross-linking methods, their advantages, and their disadvantages (**Table 1**).

Alginate, Agarose, and Gellan gum

Alginate, agarose, and gellan gum are polysaccharides that originate from non-mammalian organisms, are massively productive, and low-cost. Alginate usually extracted from the cell wall of brown algae is usually, but not always, cross-linked when it is exposed to divalent cations such as calcium. Since this cross-linking reaction is rapid, many studies have used alginate as a bioink [12]. Agarose is isolated from seaweed and has thermosensitive and reversible gelation kinetics. Low-melting-point agarose is liquefied above 60 °C and is gelled below 30 °C when the temperature decreases. Gellan gum also shows a similar gelling temperature around a physiological level, but it is determined by the addition of divalent cations, such as sodium and magnesium. In this way, the rheological and physical properties of these materials are tunable, but they do not have any sites that bind with the transmembrane proteins of human cells. Thus, many researchers have attempted modification for immobilizing arginylglycylaspartic (RGD) acids on the polysaccharide chain [36-38]. RGD modification has been demonstrated to induce better cell adhesion and proliferation for many tissue-engineering applications.

Table 1. Bioinks for 3D cell printing

Bioinks	Printing methods	Gelation mechanism	Target tissue	Cell viability	Resolution	Advantage	Disadvantage	Ref.
Alginate	Extrusion	Ionic	Cartilage	> 85%	~ 400 μm	Low cost and rapid gelation	Lack of biomimicry, low cellular adhesiveness, and limited cell proliferation and interaction	[70]
Silk fibroin	Inkjet, extrusion	Physical, enzymatic	Osteochondral tissue, human cheek	> 86%	280 - 320 μm	High mechanical properties and long-term stability	Low cellular adhesiveness	[48], [50], [51]
Collagen	Inkjet, laser, extrusion	Thermal	Liver, skin, osteochondral tissue	> 92%	45 - 60 μm (laser), ~ 500 μm (extrusion)	High cellular adhesiveness and promotion of cell migration and proliferation	Insufficient mechanical properties for structural support due to slow gelation	[23], [31], [40], [72], [91]
GelMA	Stereolithography	Photocross--linking	n/a	> 80%	6 - 17 μm	Moderate mechanical properties for structural support, high cellular adhesiveness, and promotion of cell spreading and proliferation	Potential cytotoxicity caused by UV-irradiation and low mechanical property	[28]
Fibrin	Inkjet, extrusion	Enzymatic	Heart, skin	n/a	~ 85 μm (inkjet),~ 500 μm (extrusion)	Rapid gelation, high cellular adhesiveness, and promotion of cell migration and proliferation	Insufficient mechanical properties for structural support and fast degradation	[5], [18]
PEGDA	Stereolithography	Photocross--linking	n/a	n/a	10 - 100 μm	High transparency and tunable mechanical properties	Potential cytotoxicity caused by UV-irradiation, low cellular adhesiveness, and cell proliferation	[29]
dECM	Extrusion	Thermal	Cartilage, adipose, heart, muscle,	> 95%	~ 500 μm	Suitable biomimicry, promotion of cell differentiation, proliferation, and long-term functionality.	Slow gelation, and lack of mechanical properties	[6], [7], [17], [57]
HA	Extrusion	Host-guest (receptor-ligand) interaction	Osteochondral tissue	> 86%	~ 600 μm	Promotion of cell migration and proliferation	Rapid degradation, low mechanical property, and slow gelation	[15]
Alginate--gelatin	Extrusion	Chemical (Ca^{2+})	Sweat gland, embryoid body, heart	> 81%	400 - 750 μm	Rapid gelation and extension of stable cell culture period	Rapid degradation	[77], [86], [92]
GelMA methacrylate -hyaluronic acid (GMHA)	Stereolithography	Photocross--linking	Liver	> 65%	< 10 μm	Moderate mechanical properties for structural support	Potential cytotoxicity caused by UV-irradiation	[93]
Gelatin -fibrinogen--HA-glycerol	Extrusion	Enzymatic reaction (thrombin--fibrinogen)	Bone, cartilage, skeletal muscle	> 91%	~ 400 μm	Moderate mechanical properties for structural support	Rapid degradation	[10]

Silk

Silk fibroin protein from *Bombyx mori*, the silkworm, is one of the most widely used bioinks due to its biocompatibility, robust mechanical strength, controllable degradability, and minimal inflammatory response [46]. Because of these various advantages, tissues such as cartilage, bone, and fat have been cell printed with silk fibroin bioink [47-49]. Notably, due to its remarkable long-term stability, silk fibroin constructs can maintain volume retention for over 1 year *in vivo* [47]. However, silk fibroin is not used alone in 3D cell printing because it has no lamination capacity. Thus, silk bioink is usually mixed with a thermally reversible material, such as gelatin, that can be deposited by 3D cell printing [48, 50]. The gelation of silk fibroin bioink can be induced *via* enzymatic or physical cross-linking methods. The enzymatic cross-linking method uses tyrosinase or horseradish

peroxidase (HRP), which covalently cross-links the silk polymer chain [48, 51]. On the other hand, the physical cross-linking method is dependent on the sonication that induces hydrophobic interaction and stimulates the self-assembly of silk fibroin [48]. In addition, incorporating glycerol has been reported as a new cross-linking method for silk fibroin bioink. Glycerol regulates the silk secondary structural transitions and induces the physical cross-linking of silk fibroin bioink [50]. Since incorporating glycerol is a relatively simple method of cross-linking the silk bioink compared with other methods, it is expected to be widely applied in the field of cell printing.

Collagen, Gelatin, and Fibrin

Many natural materials originating from animals have been extensively used for human cell culture and bioink formulations. Natural materials from mammalian tissues contain ECM molecules that

directly interact with cell membrane proteins and thereby exhibit inherently high bio-affinity and bio-activity. Collagen fibril is the most abundant ECM molecule in the body and is extensively used for numerous biological experiments. The precursor of collagen is the solubilized fibrils in an acid, and naturally entangles or cross-links into a hydrogel form as the temperature and pH increase to physiological levels. Additional cross-linking agents, such as n-hydroxysuccinimide and 1-ethyl-3-(3-dimethylaminopropyl)carbodiimide, can induce the irreversible polymerization of collagen. Fibrinogen is a glycoprotein that forms fibrin through a rapid reaction with thrombin to prevent loss of blood in the vessel. This rapid gelation also helps retain the 3D shape of the printed cell-laden hydrogel to achieve high shape fidelity. For example, Hinton *et al*. directly printed alginate hydrogel mixed with fibrinogen and calcium into a gelatin slurry bath containing thrombin [44]. When fibrinogen in alginate was extruded from the nozzle, it met the thrombin in the bath and rapidly polymerized to support the calcium-mediated solidification of the alginate part. Likewise, fibrinogen is widely used for a secondary gelling component in the bioink composition. Gelatin is an abundant and inexpensive material extracted from denatured collagen in animal skin and bone. It displays a reversible thermosensitive gelation mechanism that is opposite to that of collagen. Gelatin is dissolved at above 40 °C and forms random coils below 30°C. Thus, it exists in a liquid state at a physiological temperature. Some researchers have utilized this phenomenon to print a monolayer of cells with extrusion printing by washing out the liquefied gelatin post-printing [23, 52]. In contrast, other studies aim to maintain the gelatin-printed structure by methacrylation of the gelatin with irreversible UV photopolymerization [53, 54]. Gelatin–methacrylate (GelMA) hydrogels have been commonly used for laser-based cell printing [53, 54].

Poly(ethylene glycol) (PEG)

PEG is biocompatible, and the Food and Drug Administration (FDA)-approved material has been widely used in the field of regenerative medicine. In tissue printing, it has been used as a sacrificial support material that can be removed after the construction of the 3D printed structure [39]. Since PEG alone cannot generate a hydrogel, a PEG-based hydrogel should be chemically modified prior to use as a bioink. Acrylation of PEG is generally conducted for the development of a PEG-based hydrogel. Acrylated PEG is cross-linked through UV- and photoinitiator-induced photopolymerization [55]. Although mechanical properties can be tuned by adjusting the UV exposure time, this cross-linking method can reduce cell viability. Moreover, similar to alginate hydrogels, PEG-based hydrogels have an absence of cell-adhesion residues that enable cell spreading, migration, and proliferation [56]. Therefore, natural hydrogels are commonly blended with PEG-based hydrogels to improve biofunctionality, such as HA, collagen, and gelatin that have inherent bioactivity [57]. In addition, due to the biocompatibility and high transparency of PEG-based hydrogels (especially PEG diacrylate; PEGDA), they are also used for the fabrication of 3D printed bio-microfluidic devices [29, 58].

Decellularized ECM hydrogel

To better reproduce the tissue-specific complexity of original ECM, decellularization is recognized as an ideal method for preserving a specific composition including polysaccharides and proteins while avoiding immunological responses from the cellular materials [59]. An acellular tissue scaffold is normally used after recellularization with the desired cells through perfusion of the cell-suspended media into the remaining vessel network, but it is not easy to achieve heterogeneous localization with different cells. Instead, a solubilized decellularized ECM (dECM) pre-gel enables the printing of the cells following a pre-defined path by acting as a bioink. The solution can be obtained by the pepsin-mediated digestion of dECM within an acid and is solidified upon increasing the temperature and pH to physiological levels like collagen hydrogel. Therefore, it is possible to maintain the 3D structure post-printing through thermosensitive gelation kinetics. Pati *et al*. demonstrated the high cell viability of cells printed with dECM bioinks and the potential application of dECM for cell differentiation into a tissue-specific lineage. By exploiting these superior characteristics of dECM bioink, our group has pioneered the construction of living tissues with complex 3D structures as well as robust functionalities for tissue regeneration [6, 17, 60].

3D cell printed living tissue in regenerative medicine

3D cell printing of living tissues for regeneration and repair

In this section, we delineate the latest tissue constructs produced by 3D cell printing, describing their performance and regenerative capacity.

Bone tissues

Numerous studies have successfully produced 3D printed bone constructs in a defect-matched or

custom-designed manner to regenerate bone tissue [14, 61-63]. At the initial stage of bone-tissue engineering, researchers have focused on matching the mechanical properties of bone *via* the printing of synthetic materials to make 3D scaffolds [64-66]. Recently, to promote osteogenesis, many researchers have incorporated ceramic materials, such as hydroxyapatite and beta-tricalcium phosphate (β-TCP), into the 3D printed scaffolds to achieve a similar composition of native bone [67, 68]. Jakus *et al*. developed a hyperelastic bone (HB) ink that enables an elastic construct to be built for bone regeneration. They dissolved polycaprolactone (PCL) (or poly(lactic-co-glycolic acid) (PLGA)) and hydroxyapatite in a trisolvent mixture to make a HB bioink. This solvent-based osteoregenerative ink enables a surgically relevant construct to be produced that can be handled versatilely (*via* cutting, rolling, folding, suturing, etc.). They also observed that human mesenchymal stem cells (MSCs) that were seeded on HB constructs showed the significant up-regulation of pro-osteogenic genes, collagen type I, osteopontin, and osteocalcin at day 28 without any osteo-inducing factors in the medium. The HB construct was then evaluated *in vivo* in a macaque calvarial defect for 4 weeks and revealed excellent new bone formation with the vascularization and integration of surrounding tissue [62]. Although the ceramic materials provided a mineralized environment to cells and showed good bone formation capability, the complex bony ECM microenvironment that promotes the osteogenic effect could not be reproduced. Current studies have also considered recapitulating the natural bony ECM microenvironment within the 3D printed construct as well as mimicking the mineralized environment. La *et al*. developed a bone tissue substitute that replicates the micro- and mineralized environment through decellularization and demineralization. They printed PCL/PLGA/TCP scaffolds, and then coated them with the bone dECM (bdECM) that was extracted from bovine tibiae. The PCL/PLGA/TCP/bdECM scaffolds exhibited significantly enhanced calcium deposition and osteogenic gene expression. Notably, the newly formed bone was found to have almost covered the entire mouse calvarial defects through micro-CT observation. The histological analysis strongly supported the observation that over 85% of the new bone formation area and 70% of bone density was exhibited in the PCL/PLGA/TCP/bdECM scaffold (**Figure 2a**). These results demonstrate that the recapitulation of the micro- and mineralized environment of bone can significantly induce osteogenic capacity [63]. Despite this excellent regeneration capability of a 3D printed bone

substitute, the regeneration of a clinically relevant large volume of the defect is still in the early stage due to low vascularization and insufficient diffusion of oxygen and nutrients into the 3D printed constructs. Park *et al*. developed a 3D cell printed bone construct that considered both prevascularization and bone regeneration. They printed human dental pulp stem cells (DPSCs) with vascular endothelial growth factor (VEGF) in the central zone of the construct, where a hypoxic area was generated. Additionally, they also printed DPSCs with bone morphogenetic protein-2 (BMP-2) in the peripheral zone of the construct. As comparison groups, the constructs without compartments were also fabricated. The DPSCs and different growth factors were precisely placed with spatial and temporal control via 3D cell printing. No hypoxic area was generated in the entire construct, and the spatial differentiation of bone and prevasculature was observed in each area. After 4 weeks of *in vivo* evaluation, significantly higher blood vessel and bone formation were observed in both the central and peripheral zones than in the comparison groups [69]. This study indicates that 3D cell printing technology enables the construction of a large volume of vascularized tissue through the spatial distribution of cells and growth factors.

Cartilage

Although various clinical approaches such as microfracture and autologous chondrocyte implantation (ACI) have been applied to articular cartilage damage, these techniques often lead to the formation of biochemically and biomechanically inferior fibrocartilage in articular anatomy. Moreover, cartilage exhibits multiple zonal organizations with highly coordinated cell distribution. Thus, many studies have focused on developing cartilage substitutes using 3D cell printing technology for cartilage regeneration. Kundu *et al*. printed hybrid-type cartilage constructs containing chondrocyte, alginate, and PCL [70]. Park *et al*. developed 3D cell printed autologous cartilage scaffolds that consisted of autologous chondrocyte, alginate, and PCL for auricular reconstruction [16]. PCL was printed with hydrogel and cells, and it provided the construct with long-term stability [16]. Even though these constructs showed excellent chondrogenesis through *in vivo* evaluation, the abrasion of surrounding cartilage tissue might be induced due to the rigid properties of PCL. Hung *et al*. developed water-dispersible biodegradable polyurethane (PU) to make a bioink and fabricated a 3D printed cartilage construct that exhibited the high strain recovery property. Since PU can be easily dispersed in water, another bioactive compound,

including hyaluronic acid or growth factors, can be encapsulated into bioink. High glycosaminoglycan (GAG) secretion, which indicates the formation of cartilage, was observed by safranin-O staining at 4 weeks after implantation into rabbit osteochondral defects [71]. Recent studies have focused more on mimicking the multiple zonal organizations of complex cartilage environments. Lee *et al*. fabricated a 3D printed meniscus scaffold considering zone-specific meniscus regeneration. The meniscus is composed of two zones; the white zone, which is located at the inner zone of the meniscus, consists of chondrocyte-like cells with abundant GAG and collagen type II, whereas the red zone, which is in the other zone of the meniscus, contains fibroblast-like cells with collagen type I. They printed an anatomically correct meniscus scaffold and then placed human connective tissue growth factor (CTGF) in the red zone and transforming growth factor β3 (TGF β3) in the white zone. Two spatiotemporally released growth factors induced the differentiation of human synovium MSCs to form a zone-specific

matrix (white zone: collagen type II, red zone: collagen type I) in each zone. Moreover, zone-specific phenotypes were exhibited after the 3-month implantation of a sheep partial meniscectomy model [9]. Shim *et al*. developed 3D cell printed osteochondral tissue comprising bone and cartilage. It has been proven that collagen bioink has better performance for bone-tissue engineering, while hyaluronic acid bioink has a better capability for cartilage regeneration [72]. Therefore, they printed the collagen bioink containing bone morphogenetic protein-2 (BMP-2) with human nasal inferior turbinate tissue-derived mesenchymal stromal cells (hTMSCs) onto the bone part and dispensed hyaluronic acid bioink incorporating TGF β and hTMSCs to the cartilage part. With the effect of growth factors, the cells in each bioink showed significantly high osteogenic and chondrogenic gene expression in each zone, respectively. In addition, outstanding neo-cartilage and bone formation was detected in the rabbit osteochondral model (**Figure 2b**) [15].
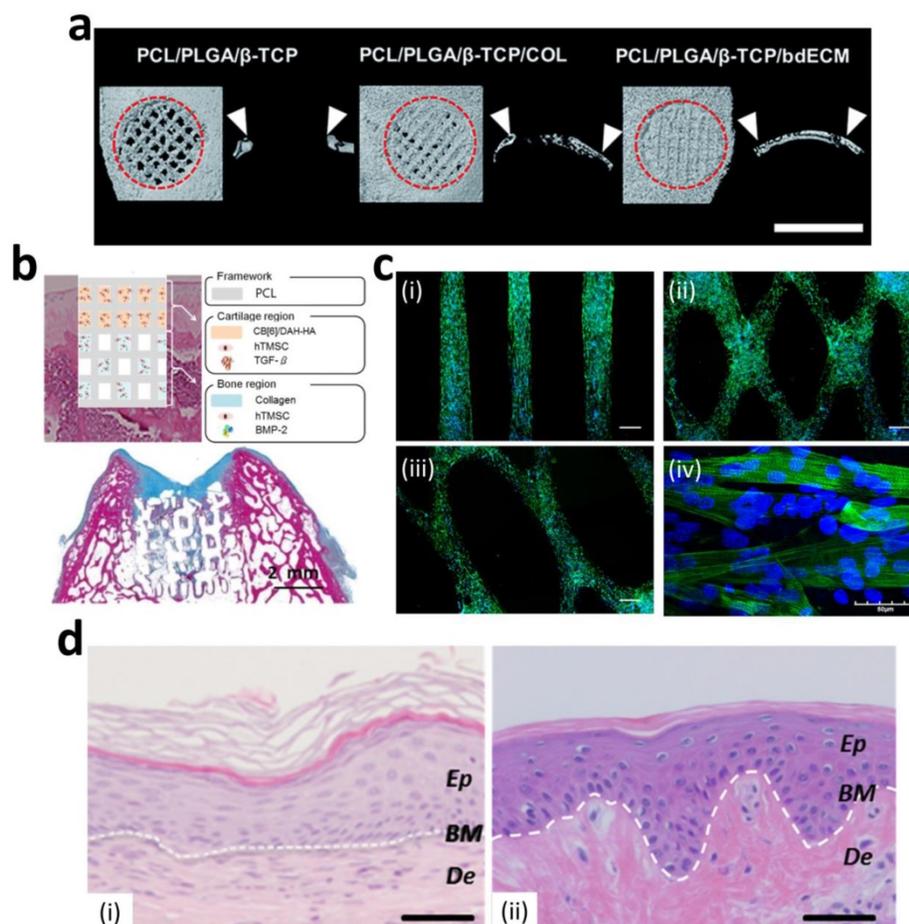

Figure 2. Regenerative capability of 3D printed tissue constructs. (a) Enhanced *in vivo* bone regeneration treated by bdECM-coated scaffolds that were evaluated *via* micro-CT (scale bars=4 mm). (b) Schematic diagram of the 3D cell printed osteochondral construct (upper) and Masson's trichrome-stained images of the construct at 8 weeks post-implantation (bottom). (c) Fluorescent images of 3D cell printed muscle construct; (i) parallel-type, (ii) diamond-type, (iii) chain-type constructs (scale bar = 200 μm), and (iv) striated muscle patterns are detected in the muscle constructs. (d) H&E staining of 3D cell printed skin grafted to immunodeficient mice (i) and normal human skin (ii) (Ep: epidermis, BM: basal membrane, De: Dermis, scale bar = 100 μm). Reproduced with permission [15, 17, 18, 63].

Cardiac and skeletal muscle

Cardiac and skeletal muscle exhibit highly organized endogenous architecture and contractile characteristics that cannot be built *via* conventional fabrication technology. Thus, 3D cell printed muscles that emulate the complex cellular orientation and bioelectrical functionality of native tissue have been fabricated for tissue regeneration. Although whole-heart fabrication is still beyond the capability of technology, many researchers have focused on the treatment of myocardial infarction (MI). Gaetani *et al.* presented a 3D cell printed cardiac patch that was fabricated with human fetal cardiomyocyte progenitor cells encapsulated in bioink for delivery to the MI region [73]. 3D cell printing enabled the generation of a cell-laden porous architecture that allowed for a sufficient supply of cellular nutrition and oxygen. Moreover, the porous 3D cell printed patch exhibited higher human fetal cardiomyocyte progenitor cell viability than did the non-porous solid construct. After printing, the patch retained its cardiogenic phenotype for up to 1 month and was successfully transplanted in a mouse MI model. The results revealed the cardiogenic patch reduced cardiac hypertrophy and fibrosis and enhanced myocardial viability [74]. Jang *et al*. developed a 3D prevascularized cardiac patch with the spatial patterning of stem cells. They used myocardial-derived bioinks extracted from the decellularization of cardiac tissue to incorporate human c-kit+ cardiac progenitor cells (hCPCs) and hTMSCs supplemented with vascular endothelial growth factor (VEGF). The two different cells were separately encapsulated in each bioink and printed with alternative patterning. After the implantation of the rat MI model, the patch promoted rapid vascularization and attenuated the negative left-ventricle remodeling with the improvement of cardiac function, implying that the 3D cell printed patch successfully delivered the cells to the right location and preserved the heart function [60].

The skeletal muscle is composed of parallel-aligned architecture and exhibits contraction in response to electrical stimulation; hence, recapitulating the architecture and function of skeletal muscle is critical for muscle regeneration. Kang *et al*. introduced a muscle construct fabricated by an integrated tissue–organ printer. They used a mixture of gelatin, fibrinogen, and hyaluronic acid hydrogel as a bioink and printed the muscle construct with C2C12 murine myoblasts. The longitudinally aligned myotubes were observed in the 3D muscle construct after day 7 of culture. The construct was ectopically and subcutaneously implanted into nude rats with an embedding common peroneal nerve (CPN) to promote integration. After 2 weeks of transplantation, well-organized muscle fibers and nerve contact, as well as improved muscle function, were observed [10]. Choi *et al*. presented a 3D functional skeletal muscle construct fabricated *via* 3D cell printing technology. The most important feature of this study was the development of muscle decellularized ECM (mdECM) bioink that provided cells with a 3D myogenic microenvironment for tissue development and maturation. The mdECM bioink showed adequate viscoelasticity and a suitable printing resolution for producing the various types of 3D cell printed muscle constructs, such as the parallel, diamond, and chain types. This indicates that the mdECM bioink can be utilized to produce the original shape of defected muscles prior to transplantation. Aligned myotubes, which exhibit striated band patterns, were observed in the construct (**Figure 2c**). In addition, the 3D cell printed muscle construct spontaneously generated visible contraction in response to electrical stimulation. This study demonstrates that a suitable microenvironment and architecture guide effective myogenic maturation [17].

Skin

Although numerous studies have tried to generate full-thickness skin substitutes, most methods are dependent on seeding methods, with which it is not easy to recapitulate the heterogeneity of skin comprising multiple types of cells. 3D cell printing allows similar tissue geometry to be built *via* the spatiotemporal pattern of various types of bioinks and cells. Pourchet *et al*. fabricated 3D cell printed full-thickness skin containing dermis and epidermis layers. They used a mixture of gelatin and fibrinogen as a bioink and printed human dermal fibroblasts with it to create a dermis construct. They then seeded the human epidermal keratinocytes on the dermis construct to generate skin substitutes with 5-mm thickness. After 26 days of culture, the 3D cell printed skin exhibited similar histological characteristics to human skin. Interestingly, high loricrin expression was also observed, indicating that the skin barrier function, which is related to the formation of the stratum corneum, had been recapitulated in the 3D cell printed skin. However, as they manually seeded the keratinocyte to make the epidermis layer, the uniform distribution of cells could not be achieved [75]. Nieves *et al*. produced a full-thickness human skin equivalent with one-step fabrication using 3D cell printing. They printed four different materials (human fibroblasts, human plasma supplemented with fibrinogen, $CaCl_2$, and human keratinocytes) within a single construct. Based on *in vitro* and *in vivo*

evaluation, highly differentiated dermis and epidermis, layers were observed, and they demonstrated that the 3D cell printed human skin equivalent was very similar to normal human skin tissue (**Figure 2d**) [18]. Recently, 3D cell printing has not only reproduced skin, but also skin appendages, such as sweat glands. The regeneration of sweat glands has not been studied in depth due to their low regenerative ability and the unknown induction niches of cellular differentiation [76]. In this regard, a suitable inductive microenvironment, as well as accurate and organized architecture, are of major importance for the specific differentiation of progenitor cells into sweat glands [77]. Huang *et al.* created a 3D ECM mimic construct for the regeneration of sweat glands. They used a mixture of plantar dermis homogenates, gelatin, and alginate supplemented with epidermal growth factor (EGF) as a bioink to foster a sweat gland-inductive microenvironment. Sweat glands were successfully formed in the 3D ECM mimic construct, and it showed its functionality through the secretion of bone morphogenetic protein 4 (BMP-4) and EGF, which play important roles in epidermal fate guidance. Interestingly, significantly enhanced sweat excretion was observed from the 3D ECM mimic construct transplanted in the burned paws of a mouse [77]. This study demonstrates that tissue-derived components retain a gland linage-inductive capability that generates functional sweat-gland tissue. As a follow-up study, Liu *et al.* investigated differentiation niche control by tailoring the architecture of a tissue construct *via* 3D cell printing technology. They found that adjusting the geometry and architecture, such as the pore size of the tissue construct, has a strong influence on guiding sweat-gland morphogenesis and function [78].

3D printing of *in vitro* tissue models

In vitro tissue models should play an important role in understanding the mechanisms of disease progression and finding a cure to overcome them. However, the conventional 2D monolayer cultures that rely on plastic dishes poorly reflect many features of the human body, such as the complex arrangement of cells, soft and elastic beds, continuous mechanical stimuli, and the various communications arising from this environment. Therefore, there is significant demand for a 3D biomimetic culture system for recreating physiologically relevant artificial tissue *in vitro*. To achieve this, 3D printing is a promising technology for generating microphysiological devices with heterogeneous tissue formations and more sophisticated functions. The printing of *in vitro* tissue

models is still at an early stage, but several attempts have demonstrated its capability for recapitulating the physiological responses of native tissues.

Micro-tissue arrays for high-throughput assay

High-throughput screening performance is an attractive feature of *in vitro* models in comparison with animal experiments. Moreover, 3D printing allows multiple micro-tissue arrays to have cellular and structural heterogeneity. The precise deposition of a single cell-laden droplet can enable the integration of multiple independent tissues with each different microenvironment into a small panel. Additionally, multiple material printing is capable of creating various combinations of different cells in a tissue on the sub-millimeter scale so that that multiple microtissues are subjected to drug candidates simultaneously. So far, few studies have demonstrated the feasibility of printing micro-tissue arrays [79, 80, 83-85].

Guermani *et al.* fabricated a microgel array to evaluate the optimal bioink type for the osteogenesis of human mesenchymal stem cells [79]. They compared hyaluronic acid (HA)-0.5% PEG, HA-1% PEG, and GelMA by repeatedly printing an array of 3 × 3 drops with 500-μm diameter on every 4 mm × 4 mm area using a commercialized "quill-pen"-like printer, SpotBot 3 (Arrayit, CA, USA) (**Figure 3a**). First, the array of four-arm PEG-acrylate microspots was deposited onto a slide glass, and then the cell-laden prepolymer thiolated HA drops were dispensed onto the microspots for HA–SH polymerization. The cell-laden GelMA droplets were positioned on a vacant area of the slide glass and cross-linked by UV irradiation. For 10 days of culture, the stem cells printed with GelMA hydrogel showed preferable osteogenic differentiation because of the higher cell viability and better adhesion in this gel type. Ma *et al.* also found the superior performance of GelMA compared with PEGDA on a screening platform [83]. Using their custom-built micro-ejection system with a solenoid valve, they printed an array of 6 × 6 hydrogel drops containing human periodontal ligament stem cells. During printing, they also adjusted the droplet size with solenoid control to generate a gradient GelMA/PEGDA ratio. They deposited the cell-laden GelMA by decreasing the volume from 400 nL to 100 nL, and then dispensed the cell-laden PEGDA onto the GelMA drops by increasing the volume from 100 nL to 400 nL. In this way, they compared the various ratios between GelMA and PEGDA after UV polymerization and concluded that GelMA had the most beneficial effect on cell viability and osteogenic differentiation.
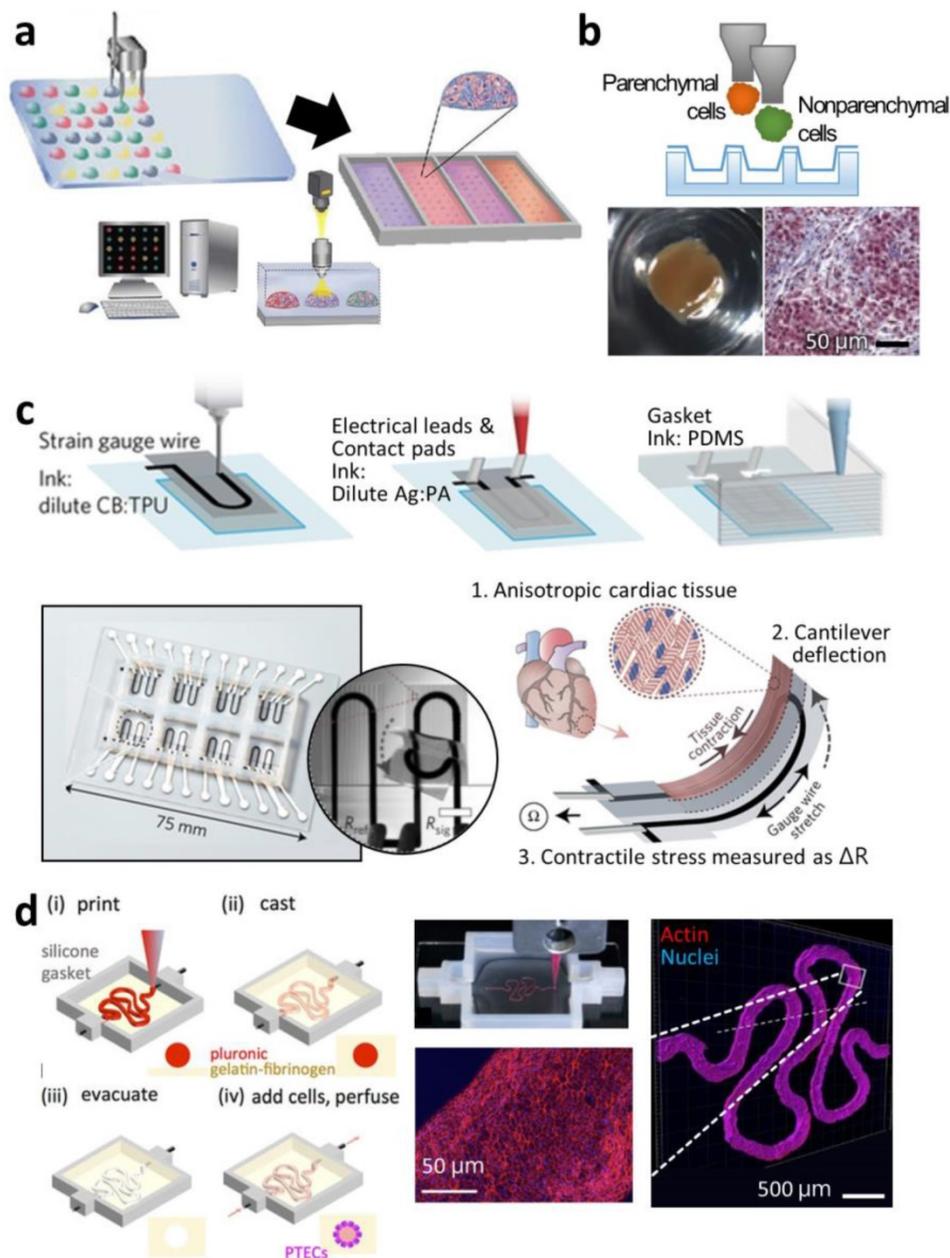
Figure 3. 3D printing of *in vitro* tissue models for finding optimal microphysiological conditions and for testing drugs. (a) Schematic diagram of the micro-gel array for a comparative study of the effects of various bioink types on stem cell differentiation into a specific lineage. (b) Images of Organovo's mini liver tissue array generated on Transwell® plate. (*Top*) Illustration of printing multiple cell types on Transwell® plate. (*Bottom*) Top-view photograph and histological observation after Masson's trichrome staining. (c) Drawings and pictures depicting the cardiomyocyte-monitoring device. (*Top*) Printing steps to incorporate electric sensors and circuits in the device. (*Bottom*) Photograph of the device with enlarged image and schematic diagram of its working principles. (d) Illustrations and images of *in vitro* kidney proximal tubule model. (*Left*) Printing steps for generating hollow tubule using fugitive ink prior to seeding of cells. (*Right*) Photograph describing the printing of fugitive ink (red) and immunofluorescent staining images to show the epithelium formation in the hollow tubule. Reproduced with permission from [79-82].

Matusaki *et al.* evaluated co-culturing environments from variously multilayered micro-liver tissues [84]. With an inkjet printer, DeskViewerTM (Cluster Technology, Osaka, Japan), they stacked a layer of human hepatocytes (Hep G2) and another layer of human umbilical vein endothelial cells (HUVEC) with different layering sequences: a monolayer of Hep G2; a double layer of HepG2-HUVEC; and a triple layer of HUVEC-HepG2-HUVEC. The micro-liver tissues of different multi-layering arrangements were produced in a 440-well plate. In the comparative study, the triple-layered tissue showed the highest albumin secretion, a hepatic marker, and the most sensitive reaction to a hepatotoxic drug, troglitazone, with decreased cell survival. Nguyen *et al.* directly dispensed NovoGel (Organovo) bioink containing HUVEC and hepatic stellate cells along the boundary of an insert well in a 24-well Transwell® plate (Corning, NY, USA), and then deposited aggregates

into the center region (**Figure 3b**) [80]. The cells in the two parts proliferated, maintaining the compartmentalized tissue formation. The multiple micro-liver tissues were tested against a non-toxic drug, levofloxacin, and a hepatotoxic drug, trovafloxacin, of varying dosages, and the printed tissues only exhibited dose-dependent sensitivity to the hepatotoxic drug. Similarly, King *et al.* developed a human breast cancer model in an insert well by printing breast cancer cell aggregates into a clump consisting of human mammary fibroblasts, human adipocytes, and HUVEC [85]. The cancer cells also showed higher chemoresistance to tamoxifen compared with those cultured in a conventional plastic dish.

Mini-tissues in meso-scale for physiological relevance

3D printing is capable of building cell-laden biological blocks with various biomaterials and facilitates the generation of artificial tissues with physiologically and/or anatomically relevant features. To create a more human-like tissue *in vitro*, various approaches have been studied, including engineering ink formulations, cell pattern and arrangement design, and configuration with other mechanical and electrical components, with the advances in printing technologies.

Ouyang *et al.* utilized a printed cell-laden hydrogel as an embryonic stem cell (ESC) cultivation system [86]. They printed a rat ESC-containing gelatin–alginate hydrogel in an 8 mm × 8mm × 1 mm lattice pattern with 500 µm-wide struts to meet the diffusion limit for oxygen (approximately 250 µm [87]) as well as provide a 3D soft environment for the ESCs using an in-house extrusion-printing system. They observed the continuous cell proliferation into spheroids while retaining the pluripotent markers, such as stage-specific embryonic antigen 1, octamer-binding transcription factor 4, and Nanog.

Gu *et al.* also printed human neuronal stem cells (hNSCs) with a polysaccharides bioink in a grid pattern to cultivate the neurons within an ECM-like microenvironment with abundant nourishment [88]. They dispensed the encapsulated cells in a mixture of alginate, carboxymethyl–chitosan, and agarose using the 3D Bioplotter System (EnvisionTEC GmbH, Gladbeck, Germany) and immersed the extruded bioink in calcium chloride solution for secondary chemical solidification. The hNSCs displayed the formation of neurite and synaptic contacts as well as bicuculline-induced calcium response. In addition to this primary neuron formation, Johnson *et al.* proposed a method for developing a systemically integrated neuron system including central and peripheral neurons, axons, and a terminal junction

[89]. Using a custom extrusion-printing system, they fabricated PCL guides on a regular culture dish and deposited grease, a silicone, in a 90°-oriented direction against the guides to construct separate chambers. Finally, three different cell suspensions were dispensed into each chamber: rat embryonic neurons isolated from the hippocampus as central neurons in chamber 1; rat embryonic neurons isolated from superior cervical ganglia as peripheral neurons and Schwann cells for sheath formation covering axons in chamber 2; and porcine kidney epithelial cells for junction formation with axon terminal ends in chamber 3. The neurons in each chamber developed neurites and axons along the PCL guides, penetrated the bottom-most grease layer, and were finally integrated into the central-peripheral neuron system. Using this system, a viral infection and its transmission were investigated. Pseudorabies virus (PRV) was inoculated to the cell body of peripheral neurons and transported to each end: another cell body of a central neuron and the terminal ends. The PRV transmission was found to be preferable to a direction toward the central neuron.

3D printing is beneficial for constructing 3D volumetric structures through the layer-by-layer process. Based on this feature, artificial skin tissues have been developed. Koch *et al.* fabricated bi-layered skin tissue composed of 20 layers of fibroblasts (NIH3T3) and another 20 layers of keratinocytes of 10 mm × 10 mm × 2 mm using a laser-assisted printing system [31]. A commercialized Matriderm® graft (MedSkin Solutions Dr. Suwelack AG, Billerbeck, Germany) composed of collagen and elastin was used as a substrate, and 20 layers of fibroblasts and 20 layers of keratinocytes were subsequently deposited on the substrate. Each layer containing fibroblasts or keratinocytes showed dermis- or epidermis-like histology, respectively. Each layer containing fibroblasts or keratinocytes showed dermis- or epidermis-like histology, respectively. Likewise, Lee *et al.* fabricated multi-layered skin tissue by the extrusion-printing method [90]. They repeatedly stacked two layers of blank collagen gel and a layer of NIH3T3 cell-laden collagen gel three to four times, and then deposited two more layers of keratinocytes over the printed construct. After two culture periods, the artificial skin tissue exhibited epithelization and stratification. Hou *et al.* attempted a transdermal penetration test of nanoparticles using a 3D printed skin model [91]. They generated skin tissue of 15 mm × 15 mm by stacking a green-labeled human dermal fibroblast-laden collagen layer and blank collagen layer using a 3D Discovery Instrument (RegenHU Ltd., Villaz-St.-Pierre, Switzerland) and polymerizing with a sodium carbonate solution. After establishing

the artificial skin tissue, they treated polystyrene nanoparticles with different surface coatings: hydroxyl, amine, and sulfate. Among these three types of nanoparticles, amine-coated polystyrene penetrated most deeply due to its positive surface charge.

Recently, 3D printing has been used for producing *in vitro* cardiac tissue models with sophisticated designs. Lind *et al*. integrated an electric sensor and circuits with a monolayer of cardiomyocytes grown on varying groove patterns by 3D printing (**Figure 3c**) [81]. The 3D printing of all the components in the *in vitro* model facilitated the real-time monitoring of the living tissue. They sequentially printed the cantilever strain gauge with carbon black-mixed ink, the circuit with silver-mixed ink, and the grooves and the gasket with silicone ink on a glass substrate, and the cells were seeded on it. When the laminar cardiac tissues on the cantilevers contracted, the deformation of sensors was transformed into electric signals and measured. In this model, the cardiac tissue displayed different contractile stresses depending on the topologic features of the grooves. Zhang *et al*. developed an endothelialized myocardium in an *in vitro* system [92]. To create the endothelium inside the cardiac tissue, they printed HUVECs with a GelMA–Alginate bioink using a commercial extrusion printer, NovoGen MMX (Organovo), and a co-axial nozzle. The inner nozzle continuously extruded the cell-laden bioink, and the outer nozzle dispensed calcium chloride for the rapid polymerization of the outside of the extruded strut. The whole construct was also irradiated with UV. After endothelium formation based on the self-assembly of the endothelial cells, cardiomyocytes were seeded on the construct and displayed cardiac maturation and sarcomeric bandings. They also evaluated the cardiovascular toxicity of an anticancer drug, doxorubicin, and this model showed dose-dependent sensitivity.

The establishment of *in vitro* liver tissue is widely studied because of its crucial role in the metabolism. Ma *et al*. focused on mimicking the anatomical cellular arrangement of liver lobules [93]. They were inspired by the hexagonal lobule unit that consists of nonparenchymal cells distributed in a radial structure and parenchymal cells occupying the main part. To mimic this structure, they used the DLP SLA technique with 5% GelMA bioink containing human-induced pluripotent stem cell-derived hepatic progenitor cells (hiPSCs–HPCs) and 25% GelMA/1% glycidal methacrylate–hyaluronic acid bioink containing HUVECs and adipose-derived stem cells (tri-culture). By sequentially shifting the digital mask, they achieved the heterogeneous tissue construction using multi-materials. The precisely printed liver tissue displayed increased albumin secretion and urea production compared with the hiPSC–HPC-only printed model and those in the 2D monolayer. Additionally, the printed liver tissue with tri-culture showed higher metabolic activity against a hepatotoxic antibiotic, rifampicin. Perfusion culture of engineered liver tissue is promising for promoting the hepatic metabolism and functions. Lee *et al*. demonstrated 3D printing of a whole construct including a perfusable microchannel and living liver tissue through a one-step fabrication process for heterogeneous tissue formation and its dynamic culture [23]. Bhise *et al*. constructed a perfusable chip device through a two-step fabrication process [94]. First, they fabricated microfluidic channels and a chamber by PDMS soft lithography, and then they directly deposited multiple hepatic spheroids in GelMA bioink in the PDMS chamber with a NovoGen extrusion printer and UV polymerization. After assembling it with other parts, the printed liver tissue was cultivated with perfusion and displayed elevated expressions of the liver-specific marker and decreasing metabolic activity with the increasing dosage of a hepatotoxic drug, acetaminophen. More importantly, Chang *et al*. presented the drug metabolism accompanying molecular change using 3D printed liver tissue [95]. They also pre-fabricated a microfluidic device with PDMS, extruded the Hep G2-laden alginate on the PDMS chamber through the in-house printing system, and assembled them together after cross-linking with calcium chloride solution. The engineered liver tissue with the perfusable channel exhibited a higher metabolic rate of 7-hydroxy-4-trifluoromethyl coumarin production from 7-ethoxy-4-trifluoromethyl coumarin compared with that in a static condition.

Selective and dynamic permeability is an important requisite characteristic in modeling a human-like tubular structure *in vitro*. To address this, Homan *et al*. attempted to generate a kidney proximal tubule with epithelium lumen and surrounding stroma with 3D printing technology [82]. For full construction *via* 3D printing, they printed a chamber with silicone on a glass, and then filled the bottom of the chamber with an ECM-like fibroblast-laden fibrinogen-gelatin-CaCl$_2$-transglutaminase solution containing fibroblasts (**Figure 3d**). After the gelation of the ECM-mimetic material, a fugitive ink, PF127, was extruded to form a convoluted proximal tubule shape, and the cell-laden ECM-mimetic material was used to fill the rest of the chamber. After the secondary gelation, each end of the tubule shape was punched and perfused with cold media. The luminal epithelium was formed by loading the cell suspension

in the tube. The engineered tubule showed diffusional permeability and its reduction due to the damage to the epithelium caused by a nephrotoxic drug, cyclosporine A, in a dose-dependent manner.

Another application of 3D printing is modeling cancer *in vitro*. Cancer is still one of the leading causes of death, and finding ways to overcome it is still an underexplored area. Therefore, it is necessary to develop artificial malignant tissue for drug development. Zhao *et al*. created human cervical cancer by printing the cancer cells with fibrinogen–gelatin–alginate bioink [96]. Since cell–ECM interactions play an important role in cancer progression, the printed cancer cells displayed the overexpression of ECM-remodeling molecules, a family of matrix metalloproteinase, and relevant morphological changes. Additionally, the printed cervical cancer showed a less sensitive response to an anticancer drug, paclitaxel, than 2D-cultured cells. Dai *et al*. also generated an *in vitro* model of glioma, a brain cancer, by extrusion printing [97]. They printed a bioink solution containing fibrinogen, transglutaminase, gelatin, and alginate with glioma stem cells in a 3D lattice pattern. The printed cancer stem cells maintained the stemness expression of nestin and exhibited better differentiation potential with an increase of glial fibrillary acidic protein and β-tubulin III. The printed glioma also showed higher drug resistance to temozolomide.

3D cell printing for theranostics applications

Although the clinical application of stem cells is still controversial, stem cells can induce a beneficial outcome associated with high proliferative capacity, paracrine effects, and pluripotent or multipotent differentiation lineages [98, 99]. When all these beneficial components are integrated, the 3D cell printed tissue equivalent has exhibited similarity in terms of the characteristics and functionality of native tissue. One of the advantages of 3D cell printing is that the functional tissue equivalent containing stem cells (as well as other cell types, e.g., progenitor cells) can be delivered in a defined manner *in vivo*. Despite the excellent regenerative capacity and original tissue-like functionality of 3D cell printed tissue equivalent, to date, few relevant studies focused on *in vivo* tracking and monitoring the therapeutic effect of 3D cell printed tissue equivalents transplanted into the defect site have been conducted. Moreover, the current methods to verify regeneration often lead to invasive techniques that cause additional pain and harm to patients [21]. Cell-labeling and tracking techniques use contrast agents, such as magnetic nanoparticles, to label specific cells to facilitate the imaging and monitoring of targeted cells, molecules, and tissues in a noninvasive and serial-tracing manner *via* imaging modalities including magnetic resonance imaging (MRI), computed tomography (CT), positron emission tomography (PET), and near-infrared (NIR) fluorescence imaging [4, 21]. Cell tracking allows the detailed monitoring of the phenomena and mechanisms involved in the therapeutic process [100, 101]. Thus, cell tracking facilitates theranostics by monitoring the site of stem cell administration and verifying cellular behavior, including viability, differentiation, and migration. Here, we suggest the potential applications of integrating cell tracking and 3D cell printing for a synergistic effect for the tissue engineering field in the near future (**Figure 4**).

Monitoring *in vivo* behavior of 3D printed scaffolds

Scaffold, mechanical, physical, and biochemical support for cells can be fabricated with defined structures via 3D printing. There are several important considerations when designing a scaffold for use in tissue regeneration. The scaffold should be biocompatible, allowing cells to adhere, proliferate, and migrate throughout the construct [102]. It should possess the appropriate mechanical properties to retain the shape of the structure and preserve the seeded cells to maintain their function from the surrounding mechanical stress *in vivo* [103]. A highly interconnected porous architecture is also important to ensure cell infiltration and diffusion of sufficient nutrients (or waste materials) and oxygen [102]. The ideal scaffold should gradually degrade as tissue regeneration progresses. Among the considerations for scaffold design, biodegradability is one of the key properties. Matching the degradation rate with tissue regeneration is problematic due to the complexity of the *in vivo* environment. Therefore, tracking the *in vivo* degradation of scaffolds as well as tissue formation in a noninvasive manner is promising for understanding the tissue regeneration process. Kim *et al*. developed NIR fluorophore (ZW800-1)-conjugated biodegradable collagen scaffolds that can be detected by NIR. They confirmed the attenuation of the NIR fluorescence signal along with scaffold degradation for 28 days in a mouse subcutaneous model as well as the absence of a toxicity effect (**Figure 5a**) [104]. Zhang *et al*. functionalized hyaluronic acid hydrogel with NIR fluorescent agent IRDye® 800CW. They observed the decay of the fluorescence signal over 7 days of *in vivo* longitudinal studies, indicating scaffold degradation [105]. Kim *et al*. focused on *in vivo* tracking of a tissue-derived scaffold. They developed a decellularized ECM scaffold for cartilage and

conjugated it with Cy3, a fluorescent dye, *via* NHS ester cross-linking reactions. They traced the scaffold for 8 weeks and found that the fluorescent signal steadily decreased as the scaffold degraded [106]. Huang *et al*. newly developed a series of tailor-made fluorescent PCL polymers. Yellow-, green-, red-, and even NIR fluorescence was represented from synthesized fluorescent PCL polymers. The degradation rate of PCL is very slow (approximately over 1 year); therefore, they tested the degradation of fluorescent PCL polymer in NaOH aqueous media. The results showed that NIR fluorescence intensity diminished consistent with the mass loss of the scaffold over one week, implying the degradation result was monitored by NIR fluorescence [107]. Since PCL has been widely used in biomedical applications, including 3D printing, it is a promising material for tissue regeneration applications.

Figure 4. Schematic illustration of 3D cell printing for theranostics applications.

Monitoring the *in vitro* tissue model

The development cost of new pharmaceuticals is extremely high and is increasing each year. Even though animal models have been utilized for drug screening and toxicology applications due to their physiological relevance and reflection of organ-level interactions, these models are costly, time-consuming, and raise ethical concerns [108]. Moreover, animal testing for cosmetics has been completely banned since 2013 [109]. In addition, drug efficacy and tolerability can vary significantly by individual; therefore, personalized therapy has been conducted according to the patient's genetic profile or using patient-derived samples. While patient profiling and patient samples can improve outcomes, uncertainty and low throughput are major hurdles for personalized therapy [110]. In this regard, the development of an alternative test platform that exhibits physiological compatibility or the patient's pathological phenotype is considered to be challenging, but urgently needed. As described above, 3D cell printing can generate 3D tissue-like structures that replicate the function and characteristics of native tissue. Moreover, if autologous cells or patient-derived induced pluripotent stem cells are used, patient-specific tissue or pathological models can be produced through 3D cell printing [93]. Of course, the development of an *in vitro* model through 3D cell printing is still in the early stage, but numerous 3D cell printed *in vitro* models have been produced, some of which show similar performance to that of the original tissue [81, 82, 88, 92]. However, since 3D cell printing generates large volumetric constructs, elucidating the cellular behavior, regenerative capacity (or disease progression), and functionality of 3D cell printed tissue models in a noninvasive and real-time manner is difficult through typical imaging techniques due to their low resolution and poor imaging penetration. The study conducted by Chung *et al*. can directly give inspiration to overcome this problem. They treated gold nanotracers (GNT) with adipose-derived stem cells (ASCs), and then GNT-loaded ASCs were encapsulated in PEGylated fibrin hydrogel. They monitored the ASCs in the 3D hydrogel construct through ultrasound and photoacoustic imaging at each time point without sacrificing the
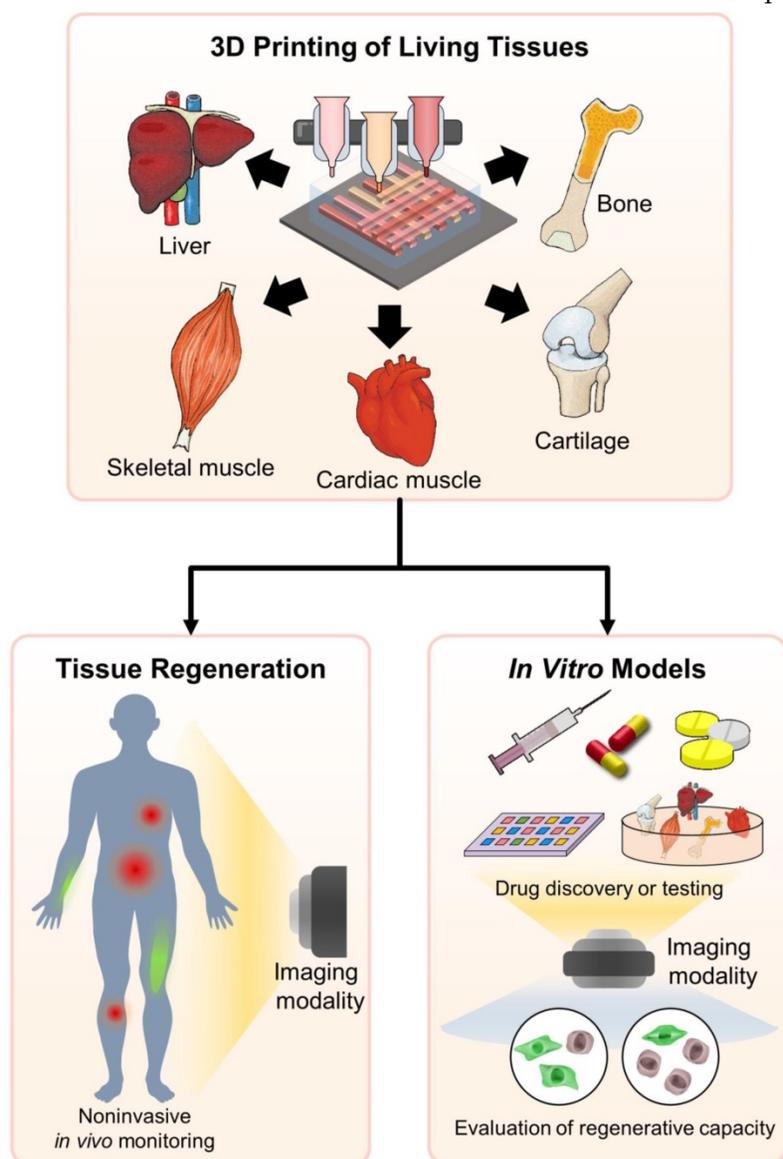
samples [111]. This study suggests that the cell-tracking technique offers advantages over the 3D printed *in vitro* model in terms of noninvasively monitoring cellular activity, including the regenerative or disease process, viability, differentiation, and functionality. The 3D cell printed tissue model can be adapted for other purposes. Hou *et al.* produced a 3D cell printed skin model for the examination of the transdermal penetration capability of nanoparticles [91]. This study suggests that the 3D cell printed *in vitro* model could be applied to verify the delivery or imaging efficacy of newly developed therapeutic or fluorescent nanoparticles.

In vivo tracking of 3D cell printed tissue

Despite the great regenerative potency of 3D cell printing, it is difficult to establish the ideal time point for transplantation of the tissue construct to the lesion site. This complication is associated with sample sacrifices, which requires significant amounts of money and time. Moreover, it is hard to trace the *in vivo* fate of transplanted tissue constructs without a noninvasive method. Nanoparticle-based cell tracking has successfully offered the noninvasive and real-time monitoring of cells delivered to injured and pathologic regions [21]. For example, tracking the stem cells delivered to the MI model through nanoparticles, such as superparamagnetic iron oxide nanoparticles (SPIONs), has been extensively studied [112-114]. Nonetheless, nanoparticle-based cell tracking is not easily applicable to *in vivo* monitoring for evaluating tissue reconstruction. Recently developed NIR fluorophores have allowed *in vivo*

imaging of specific tissues, including bone, cartilage, and the thyroid gland (**Figure 5b**) [115-119]. These fluorophores use an affinity for molecules existing in the tissue [116]. Bisphosphonates exhibit high affinity for minerals and calcium salts that are present on the bone surface. However, the molecular targets of some of these fluorophores remain unknown [118]. The NIR fluorophores suggest that this imaging technique could evaluate the regeneration capability of 3D cell printed constructs *in vitro* and allow *in vivo* monitoring of the regenerated area where the 3D cell printed construct was transplanted. Furthermore, this could be applied to selectively visualize heterogeneous tissue, such as osteochondral tissue, tendon to muscle (or bone) insertion [15, 120]. Finally, a combination of nanoparticle-based cell tracking and NIR fluorophore-based tissue imaging would be a powerful tool for monitoring the fate and regenerative capability of 3D cell printed tissue constructs.

Future perspectives

For decades, 3D cell printing technology has been steadily advancing, and fabricated tissues have shown remarkable regenerative capabilities. The integration of 3D cell printing with stem cell theranostics holds significant promise in the field of tissue engineering. More specifically, theranostics can be applied to track the degradation of fabricated scaffolds and monitor the performance of printed tissues *in vitro* as well as *in vivo*. Despite significant progress, several hurdles must be addressed to bridge the bench-to-bedside translation gap.
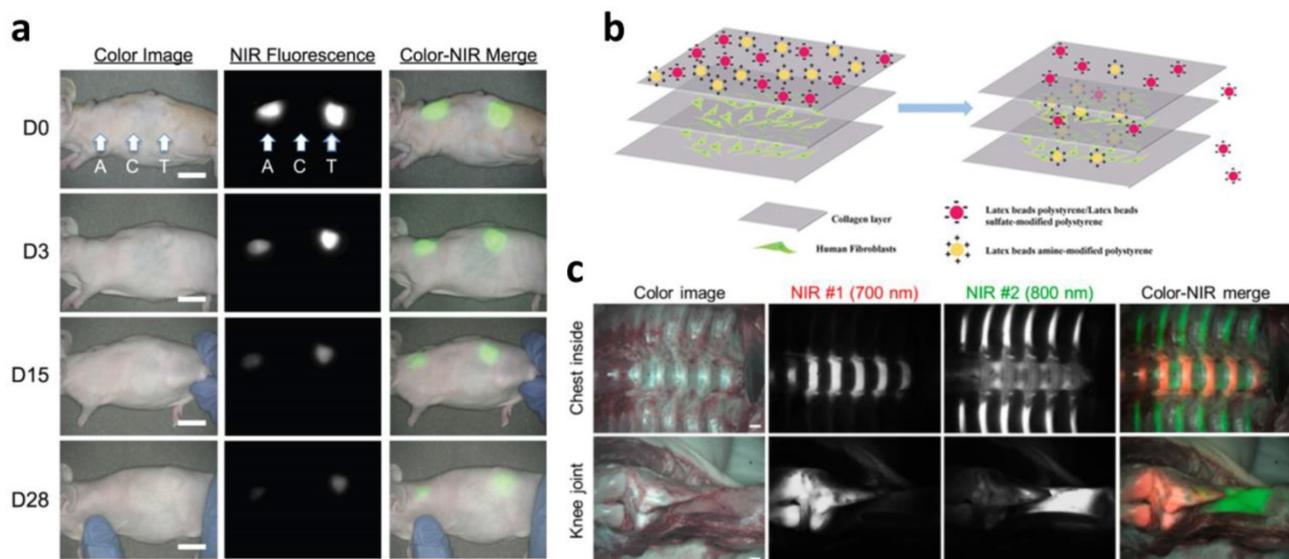

Figure 5. *In vivo* and *in vitro* monitoring of scaffolds and tissues. (a) Monitoring scaffold degradation through imaging NIR fluorescence over the skin. A, axilla; C, control; T, thigh (scale bars = 1 cm). (b) *In vivo* performance of NIR fluorophores that target specific tissues (scale bars = 1 cm). Reproduced with permission [91, 104, 116].

High cell viability is a crucial prerequisite for the 3D cell printing process. Although many printed tissues have shown over 90% cell viability, most of these tissues were smaller than even a part of a human organ. In order to maintain cell viability in large-volume tissue constructs several new methods have been proposed. Since the 3D cell printing process usually involves harsh conditions that can induce dehydration and contamination of the bioink, a closed chamber system is commonly implemented to maintain a sterile and humid environment [20, 121-123]. The construction of large-volume tissues usually takes a long time, which decreases cell viability and therefore results in insufficient functionality. Lee *et al*. reported that the construction of large-volume tissues at low temperatures (6°C) can maintain high cell viability even for a lengthy printing process [123]. Another problem in the production of large 3D cell-printed tissues is their limited capacity for diffusion that can hinder the delivery of sufficient oxygen and nutrients, leading to hypoxia and cell death [52]. To promote the transfer of oxygen and nutrients, Kang *et al*. have incorporated interconnected polymeric frameworks between printed cell struts [10], and Kolesky *et al*. have introduced perfusable vessels into thick tissue constructs [124]. Interconnected porosity and vascularization will be instrumental in maintaining high viability and functionality in large 3D cell printed tissues. Although the fabrication of large-volume tissue constructs is crucially important for generating physiologically relevant tissue, few research attempts have been made, and more advanced technologies are still required.

Since human organs and tissues are composed of various cell types in specific locations, tissues should be engineered to comprise multiple cell types with consistent spatial organization. However, the induction of multiple types of cell differentiation in a tissue construct is not trivial as there are challenges involved in establishing optimal co-culture media composition. Although a combination of several differentiation media has been used for culturing engineered tissue containing multiple types of cells, if the components of the media are not carefully selected, incomplete maturation or unintended differentiation of the cells can occur [125-128]. Recent studies have demonstrated that tissue-specific dECM bioinks (e.g., for heart, adipose, cartilage, liver, or muscle tissue) provide suitable microenvironments for promoting the growth and differentiation of cells into tissue-specific lineages [6]. Therefore, spatially directed printing of tissue-specific dECM bioinks will offer spatial inductive cues that direct each cell to differentiate into the desired tissue-specific lineage,

capitalizing on the intrinsic capability of the right kinds of cells to assemble into physiologically relevant tissue.

Although existing bioinks resemble the 3D ECM microenvironment that affects cellular processes, including migration, behavior, and differentiation, the development of an ideal bioink that meets both the physical and biological requirements of cells is still necessary. This bioink should have enough resolution and shape fidelity to replicate the microstructure of natural tissue. However, bioinks with the appropriate resolution and mechanical properties are associated with high viscosity and cross-linking density that can result in low cellular activity [43]. A tissue construct with poor mechanical properties cannot maintain its shape *in vitro* or *in vivo* and is hard to handle during implantation. Recent research has demonstrated that cells secreting ECM components can enhance the mechanical integrity of tissue constructs [17, 129, 130]. Therefore, a bioink or bio-reacting system that can stimulate these cells mechanically, chemically, or electrically should be developed to accelerate the secretion of ECM molecules. Nevertheless, it is still difficult to achieve mechanical properties similar to those, for example, of the titanium implants used for bone reconstruction. A hybrid structure comprising polymeric frameworks with cell-encapsulated hydrogels have been fabricated to improve the mechanical properties of tissue constructs [40, 70]. Once the first layer of polymeric framework is fabricated, the cell-encapsulated hydrogel is infused into the channels of the polymeric framework, and then the second framework is re-deposited onto the construct in a layer-by-layer process. The polymeric framework serves as mechanical support for the cell-encapsulated hydrogel in order to maintain cellular function. Although biodegradable synthetic polymers exhibit various mechanical and degradation kinetics, the selection of polymers appropriate for these frameworks is generally limited due to high melting temperatures (above 100°C) that can cause thermal damage to the cells. Kim *et al*. have suggested creating a protective layer against thermal damage by depositing PCL, which has a low melting temperature (60°C), onto the PLGA or polylactic acid (PLA) frameworks containing the cell-encapsulated hydrogel [131]. This approach will broaden the set of polymers acceptable for use in 3D cell printing, thereby facilitating greater control of the degradation rate and fabrication of hard tissues, as well soft tissues where an elastic polymer such as PU may be effective.

Cell printing systems, bioinks and their outcomes are associated with critical concerns regarding potential adverse effects, including an excessive immune response and insufficient

functionality of printed tissues. Therefore, all aspects of the cell printing process should follow the regulatory guidelines for clinical use. As aforementioned, integration of 3D cell printing and theranostics allows the noninvasive tracking of cellular activity in the tissue constructs. Therefore, it can be applied as a tool for investigating the performance of 3D cell printed tissue constructs before they are implanted. It can be further applied to verify the *in vivo* characteristics of fabricated tissues, such as their safety and regeneration capability. This approach may help to close the translation gap in 3D cell printing technology, allowing fabricated tissue constructs to be available for clinical use in the near future.

Acknowledgements

Competing Interests

The authors have declared that no competing interest exists.

References

1. Zimmermann W-H, Melnychenko I, Wasmeier G, Didie M, Naito H, Nixdorff U, et al. Engineered heart tissue grafts improve systolic and diastolic function in infarcted rat hearts. Nature Medicine. 2006; 12: 452-8.
2. Liechty KW, MacKenzie TC, Shaaban AF, Radu A, Moseley AB, Deans R, et al. Human mesenchymal stem cells engraft and demonstrate site-specific differentiation after in utero transplantation in sheep. Nature Medicine. 2000; 6: 1282-6.
3. Li L, Jiang W, Luo K, Song H, Lan F, Wu Y, et al. Superparamagnetic iron oxide nanoparticles as MRI contrast agents for non-invasive stem cell labeling and tracking. Theranostics. 2013; 3: 595-615.
4. Wang Y, Xu C, Ow H. Commercial nanoparticles for stem cell labeling and tracking. Theranostics. 2013; 3: 544-60.
5. Coulombe KL, Bajpai VK, Andreadis ST, Murry CE. Heart regeneration with engineered myocardial tissue. Annual Review of Biomedical Engineering. 2014; 16: 1-28.
6. Pati F, Jang J, Ha D-H, Won Kim S, Rhie J-W, Shim J-H, et al. Printing three-dimensional tissue analogues with decellularized extracellular matrix bioink. Nature Communications. 2014; 5: 3935.
7. Pati F, Ha D-H, Jang J, Han HH, Rhie J-W, Cho D-W. Biomimetic 3D tissue printing for soft tissue regeneration. Biomaterials. 2015; 62: 164-75.
8. Mironov V, Reis N, Derby B. Review: bioprinting: a beginning. Tissue Engineering. 2006; 12: 631-4.
9. Lee CH, Rodeo SA, Fortier LA, Lu C, Erisken C, Mao JJ. Protein-releasing polymeric scaffolds induce fibrochondrocytic differentiation of endogenous cells for knee meniscus regeneration in sheep. Science Translational Medicine. 2014; 6: 266ra171-266ra171.
10. Kang H-W, Lee SJ, Ko IK, Kengla C, Yoo JJ, Atala A. A 3D bioprinting system to produce human-scale tissue constructs with structural integrity. Nature Biotechnology. 2016; 34: 312-9.
11. Mandrycky C, Wang Z, Kim K, Kim D-H. 3D bioprinting for engineering complex tissues. Biotechnology Advances. 2016; 34: 422-34.
12. Axpe E, Oyen ML. Applications of alginate-based bioinks in 3D bioprinting. International Journal of Molecular Sciences. 2016; 17: 1976.
13. Arslan-Yildiz A, El Assal R, Chen P, Guven S, Inci F, Demirci U. Towards artificial tissue models: past, present, and future of 3D bioprinting. Biofabrication. 2016; 8: 014103.
14. Pati F, Song T-H, Rijal G, Jang J, Kim SW, Cho D-W. Ornamenting 3D printed scaffolds with cell-laid extracellular matrix for bone tissue regeneration. Biomaterials. 2015; 37: 230-41.
15. Shim J-H, Jang K-M, Hahn SK, Park JY, Jung H, Oh K, et al. Three-dimensional bioprinting of multilayered constructs containing human mesenchymal stromal cells for osteochondral tissue regeneration in the rabbit knee joint. Biofabrication. 2016; 8: 014102.
16. Park JY, Choi Y-J, Shim J-H, Park JH, Cho D-W. Development of a 3D cell printed structure as an alternative to autologs cartilage for auricular reconstruction. Journal of Biomedical Materials Research Part B: Applied Biomaterials. 2016.
17. Choi Y-J, Kim TG, Jeong J, Yi H-G, Park JW, Hwang W, et al. 3D Cell printing of Functional Skeletal Muscle Constructs Using Skeletal Muscle-Derived Bioink. Advanced Healthcare Materials. 2016; 5: 2636-45.
18. Nieves C, Marta G, Juan FdC, Diego V, Jose LJ. 3D bioprinting of functional human skin: production and in vivo analysis. Biofabrication. 2017; 9: 015006.
19. Jang J, Yi H-G, Cho D-W. 3D Printed Tissue Models: Present and Future. ACS Biomaterials Science & Engineering. 2016; 2: 1722-31.
20. Murphy SV, Atala A. 3D bioprinting of tissues and organs. Nature Biotechnology. 2014; 32: 773-85.
21. Edmundson M, Thanh NT, Song B. Nanoparticles based stem cell tracking in regenerative medicine. Theranostics. 2013; 3: 573-82.
22. Hull CW. Apparatus for production of three-dimensional objects by stereolithography. US Patent. 1986; US4575330A.
23. Lee H, Cho D-W. One-step fabrication of an organ-on-a-chip with spatial heterogeneity using a 3D bioprinting technology. Lab on a Chip. 2016; 16: 2618-25.
24. Xing J-F, Zheng M-L, Duan X-M. Two-photon polymerization microfabrication of hydrogels: an advanced 3D printing technology for tissue engineering and drug delivery. Chemical Society Reviews. 2015; 44: 5031-9.
25. Gissibl T, Thiele S, Herkommer A, Giessen H. Two-photon direct laser writing of ultracompact multi-lens objectives. Nature Photonics. 2016; 10: 554-60.
26. Gittard SD, Ovsianikov A, Akar H, Chichkov B, Monteiro-Riviere NA, Stafslien S, et al. Two Photon Polymerization-Micromolding of Polyethylene Glycol-Gentamicin Sulfate Microneedles. Advanced Engineering Materials. 2010; 12: B77-B82.
27. Bhattacharjee N, Urrios A, Kang S, Folch A. The upcoming 3D-printing revolution in microfluidics. Lab on a Chip. 2016; 16: 1720-42.
28. Soman P, Chung PH, Zhang AP, Chen S. Digital microfabrication of user-defined 3D microstructures in cell-laden hydrogels. Biotechnology and Bioengineering. 2013; 110: 3038-47.
29. Liu J, Hwang HH, Wang P, Whang G, Chen S. Direct 3D-printing of cell-laden constructs in microfluidic architectures. Lab on a Chip. 2016; 16: 1430-8.
30. Guillotin B, Souquet A, Catros S, Duocastella M, Pippenger B, Bellance S, et al. Laser assisted bioprinting of engineered tissue with high cell density and microscale organization. Biomaterials. 2010; 31: 7250-6.
31. Koch L, Deiwick A, Schlie S, Michael S, Gruene M, Coger V, et al. Skin tissue generation by laser cell printing. Biotechnology and Bioengineering. 2012; 109: 1855-63.
32. Roth EA, Xu T, Das M, Gregory C, Hickman JJ, Boland T. Inkjet printing for high-throughput cell patterning. Biomaterials. 2004; 25: 3707-15.
33. Calvert P. Inkjet Printing for Materials and Devices. Chemistry of Materials. 2001; 13: 3299-305.
34. Chang CC, Boland ED, Williams SK, Hoying JB. Direct-write bioprinting three-dimensional biohybrid systems for future regenerative therapies. Journal of Biomedical Materials Research Part B: Applied Biomaterials. 2011; 98B: 160-70.
35. Groll J, Boland T, Blunk T, Burdick JA, Cho D-W, Dalton PD, et al. Biofabrication: reappraising the definition of an evolving field. Biofabrication. 2016; 8: 013001.
36. Teo EY, Ong S-Y, Khoon Chong MS, Zhang Z, Lu J, Moochhala S, et al. Polycaprolactone-based fused deposition modeled mesh for delivery of antibacterial agents to infected wounds. Biomaterials. 2011; 32: 279-87.
37. Yi H-G, Choi Y-J, Kang KS, Hong JM, Pati RG, Park MN, et al. A 3D-printed local drug delivery patch for pancreatic cancer growth suppression. Journal of Controlled Release. 2016; 238: 231-41.
38. Park JH, Jang J, Lee JS, Cho D-W. Current advances in three-dimensional tissue/organ printing. Tissue Engineering and Regenerative Medicine. 2016; 13: 612-21.
39. Park JH, Jang J, Lee J-S, Cho D-W. Three-dimensional printing of tissue/organ analogues containing living cells. Annals of Biomedical Engineering. 2017; 45: 180-94.
40. Lee JW, Choi Y-J, Yong W-J, Pati F, Shim J-H, Kang KS, et al. Development of a 3D cell printed construct considering angiogenesis for liver tissue engineering. Biofabrication. 2016; 8: 015007.
41. Jung JW, Lee J-S, Cho D-W. Computer-aided multiple-head 3D printing system for printing of heterogeneous organ/tissue constructs. Scientific Reports. 2016; 6: 21685.
42. Yi H-G, Kang KS, Hong JM, Jang J, Park MN, Jeong YH, et al. Effects of electromagnetic field frequencies on chondrocytes in 3D cell-printed composite constructs. Journal of Biomedical Materials Research Part A. 2016; 104: 1797-804.
43. Malda J, Visser J, Melchels FP, Jüngst T, Hennink WE, Dhert WJ, et al. 25th anniversary article: engineering hydrogels for biofabrication. Advanced Materials. 2013; 25: 5011-28.
44. Hinton TJ, Jallerat Q, Palchesko RN, Park JH, Grodzicki MS, Shue H-J, et al. Three-dimensional printing of complex biological structures by freeform reversible embedding of suspended hydrogels. Science Advances. 2015; 1.
45. Hinton TJ, Hudson A, Pusch K, Lee A, Feinberg AW. 3D Printing PDMS Elastomer in a Hydrophilic Support Bath via Freeform Reversible Embedding. ACS Biomaterials Science & Engineering. 2016; 2: 1781-6.

46. Kundu B, Rajkhowa R, Kundu SC, Wang X. Silk fibroin biomaterials for tissue regenerations. Advanced Drug Delivery Reviews. 2013; 65: 457-70.

47. Bellas E, Panilaitis BJB, Glettig DL, Kirker-Head CA, Yoo JJ, Marra KG, et al. Sustained volume retention in vivo with adipocyte and lipoaspirate seeded silk scaffolds. Biomaterials. 2013; 34: 2960-8.

48. Das S, Pati F, Choi Y-J, Rijal G, Shim J-H, Kim SW, et al. Bioprintable, cell-laden silk fibroin–gelatin hydrogel supporting multilineage differentiation of stem cells for fabrication of three-dimensional tissue constructs. Acta Biomaterialia. 2015; 11: 233-46.

49. Melke J, Midha S, Ghosh S, Ito K, Hofmann S. Silk fibroin as biomaterial for bone tissue engineering. Acta Biomaterialia. 2016; 31: 1-16.

50. Rodriguez MJ, Brown J, Giordano J, Lin SJ, Omenetto FG, Kaplan DL. Silk based bioinks for soft tissue reconstruction using 3-dimensional (3D) printing with in vitro and in vivo assessments. Biomaterials. 2017; 117: 105-15.

51. Tao H, Marelli B, Yang M, An B, Onses MS, Rogers JA, et al. Inkjet Printing of Regenerated Silk Fibroin: From Printable Forms to Printable Functions. Advanced Materials. 2015; 27: 4273-9.

52. Lee VK, Kim DY, Ngo H, Lee Y, Seo L, Yoo S-S, et al. Creating perfused functional vascular channels using 3D bio-printing technology. Biomaterials. 2014; 35: 8092-102.

53. Yue K, Trujillo-de Santiago G, Alvarez MM, Tamayol A, Annabi N, Khademhosseini A. Synthesis, properties, and biomedical applications of gelatin methacryloyl (GelMA) hydrogels. Biomaterials. 2015; 73: 254-71.

54. Gauvin R, Chen Y-C, Lee JW, Soman P, Zorlutuna P, Nichol JW, et al. Microfabrication of complex porous tissue engineering scaffolds using 3D projection stereolithography. Biomaterials. 2012; 33: 3824-34.

55. Hospodiuk M, Dey M, Sosnoski D, Ozbolat IT. The bioink: A comprehensive review on bioprintable materials. Biotechnology Advances. 2017.

56. Moon JJ, Saik JE, Poche RA, Leslie-Barbick JE, Lee S-H, Smith AA, et al. Biomimetic hydrogels with pro-angiogenic properties. Biomaterials. 2010; 31: 3840-7.

57. Jia W, Gungor-Ozkerim PS, Zhang YS, Yue K, Zhu K, Liu W, et al. Direct 3D bioprinting of perfusable vascular constructs using a blend bioink. Biomaterials. 2016; 106: 58-68.

58. Urrios A, Parra-Cabrera C, Bhattacharjee N, Gonzalez-Suarez AM, Rigat-Brugarolas LG, Nallapatti U, et al. 3D-printing of transparent bio-microfluidic devices in PEG-DA. Lab on a Chip. 2016; 16: 2287-94.

59. Ott HC, Matthiesen TS, Goh S-K, Black LD, Kren SM, Netoff TI, et al. Perfusion-decellularized matrix: using nature's platform to engineer a bioartificial heart. Nature Medicine. 2008; 14: 213-21.

60. Jang J, Park H-J, Kim S-W, Kim H, Park JY, Na SJ, et al. 3D printed complex tissue construct using stem cell-laden decellularized extracellular matrix bioinks for cardiac repair. Biomaterials. 2017; 112: 264-74.

61. Daly AC, Cunniffe GM, Sathy BN, Jeon O, Alsberg E, Kelly DJ. 3D Bioprinting of Developmentally Inspired Templates for Whole Bone Organ Engineering. Advanced Healthcare Materials. 2016; 5: 2353-62.

62. Jakus AE, Rutz AL, Jordan SW, Kannan A, Mitchell SM, Yun C, et al. Hyperelastic "bone": A highly versatile, growth factor–free, osteoregenerative, scalable, and surgically friendly biomaterial. Science Translational Medicine. 2016; 8: 358ra127-358ra127.

63. La W-G, Jang J, Kim BS, Lee MS, Cho D-W, Yang HS. Systemically replicated organic and inorganic bony microenvironment for new bone formation generated by a 3D printing technology. RSC Advances. 2016; 6: 11546-53.

64. Hutmacher DW. Scaffolds in tissue engineering bone and cartilage. Biomaterials. 2000; 21: 2529-43.

65. Williams JM, Adewunmi A, Schek RM, Flanagan CL, Krebsbach PH, Feinberg SE, et al. Bone tissue engineering using polycaprolactone scaffolds fabricated via selective laser sintering. Biomaterials. 2005; 26: 4817-27.

66. Hollister SJ. Porous scaffold design for tissue engineering. Nature Materials. 2005; 4: 518-24.

67. Tan K, Chua C, Leong K, Cheah C, Cheang P, Bakar MA, et al. Scaffold development using selective laser sintering of polyetheretherketone–hydroxyapatite biocomposite blends. Biomaterials. 2003; 24: 3115-23.

68. Mondrinos MJ, Dembzynski R, Lu L, Byrapogu VK, Wootton DM, Lelkes PI, et al. Porogen-based solid freeform fabrication of polycaprolactone–calcium phosphate scaffolds for tissue engineering. Biomaterials. 2006; 27: 4399-408.

69. Park JY, Shim J-H, Choi S-A, Jang J, Kim M, Lee SH, et al. 3D printing technology to control BMP-2 and VEGF delivery spatially and temporally to promote large-volume bone regeneration. Journal of Materials Chemistry B. 2015; 3: 5415-25.

70. Kundu J, Shim J-H, Jang J, Kim S-W, Cho D-W. An additive manufacturing-based PCL–alginate–chondrocyte bioprinted scaffold for cartilage tissue engineering. Journal of Tissue Engineering and Regenerative Medicine. 2015; 9: 1286-97.

71. Hung K-C, Tseng C-S, Dai L-G, Hsu S-h. Water-based polyurethane 3D printed scaffolds with controlled release function for customized cartilage tissue engineering. Biomaterials. 2016; 83: 156-68.

72. Park JY, Choi J-C, Shim J-H, Lee J-S, Park H, Kim SW, et al. A comparative study on collagen type I and hyaluronic acid dependent cell behavior for osteochondral tissue bioprinting. Biofabrication. 2014; 6: 035004.

73. Gaetani R, Doevendans PA, Metz CHG, Alblas J, Messina E, Giacomello A, et al. Cardiac tissue engineering using tissue printing technology and human cardiac progenitor cells. Biomaterials. 2012; 33: 1782-90.

74. Gaetani R, Feyen DAM, Verhage V, Slaats R, Messina E, Christman KL, et al. Epicardial application of cardiac progenitor cells in a 3D-printed gelatin/hyaluronic acid patch preserves cardiac function after myocardial infarction. Biomaterials. 2015; 61: 339-48.

75. Pourchet LJ, Thepot A, Albouy M, Courtial EJ, Boher A, Blum LJ, et al. Human Skin 3D Bioprinting Using Scaffold-Free Approach. Advanced Healthcare Materials. 2016: 1601101-n/a.

76. Lu Catherine P, Polak L, Rocha Ana S, Pasolli HA, Chen S-C, Sharma N, et al. Identification of Stem Cell Populations in Sweat Glands and Ducts Reveals Roles in Homeostasis and Wound Repair. Cell. 2012; 150: 136-50.

77. Huang S, Yao B, Xie J, Fu X. 3D bioprinted extracellular matrix mimics facilitate directed differentiation of epithelial progenitors for sweat gland regeneration. Acta Biomaterialia. 2016; 32: 170-7.

78. Liu N, Huang S, Yao B, Xie J, Wu X, Fu X. 3D bioprinting matrices with controlled pore structure and release function guide in vitro self-organization of sweat gland. Scientific Reports. 2016; 6: 34410.

79. Guermani E, Shaki H, Mohanty S, Mehrali M, Arpanaei A, Gaharwar AK, et al. Engineering complex tissue-like microgel arrays for evaluating stem cell differentiation. Scientific Reports. 2016; 6: 30445.

80. Nguyen DG, Funk J, Robbins JB, Crogan-Grundy C, Presnell SC, Singer T, et al. Bioprinted 3D Primary Liver Tissues Allow Assessment of Organ-Level Response to Clinical Drug Induced Toxicity In Vitro. PloS one. 2016; 11: e0158674.

81. Lind JU, Busbee TA, Valentine AD, Pasqualini FS, Yuan H, Yadid M, et al. Instrumented cardiac microphysiological devices via multimaterial three-dimensional printing. Nature Materials. 2017; 16: 303-8.

82. Homan KA, Kolesky DB, Skylar-Scott MA, Herrmann J, Obuobi H, Moisan A, et al. Bioprinting of 3D Convoluted Renal Proximal Tubules on Perfusable Chips. Scientific Reports. 2016; 6: 34845.

83. Ma Y, Ji Y, Huang G, Ling K, Zhang X, Xu F. Bioprinting 3D cell-laden hydrogel microarray for screening human periodontal ligament stem cell response to extracellular matrix. Biofabrication. 2015; 7: 044105.

84. Matsusaki M, Sakaue K, Kadowaki K, Akashi M. Three-Dimensional Human Tissue Chips Fabricated by Rapid and Automatic Inkjet Cell Printing. Advanced Healthcare Materials. 2013; 2: 534-9.

85. King SM, Gorgen V, Presnell SC, Nguyen DG, Shepherd BR, Ridge N. Development of 3D bioprinted human breast cancer for in vitro screening of therapeutics targeted against cancer progression. American Soceity of Biology, New Orleans, LA. 2013.

86. Ouyang L, Yao R, Mao S, Chen X, Na J, Sun W. Three-dimensional bioprinting of embryonic stem cells directs highly uniform embryoid body formation. Biofabrication. 2015; 7: 044101.

87. Zhu W, Kato Y, Artemov D. Heterogeneity of tumor vasculature and antiangiogenic intervention: insights from MR angiography and DCE-MRI. PloS one. 2014; 9: e86583.

88. Gu Q, Tomaskovic-Crook E, Lozano R, Chen Y, Kapsa RM, Zhou Q, et al. Functional 3D Neural Mini-Tissues from Printed Gel-Based Bioink and Human Neural Stem Cells. Advanced Healthcare Materials. 2016; 5: 1429-38.

89. Johnson BN, Lancaster KZ, Hogue IB, Meng F, Kong YL, Enquist LW, et al. 3D printed nervous system on a chip. Lab on a Chip. 2016; 16: 1393-400.

90. Lee V, Singh G, Trasatti JP, Bjornsson C, Xu X, Tran TN, et al. Design and fabrication of human skin by three-dimensional bioprinting. Tissue Engineering Part C: Methods. 2013; 20: 473-84.

91. Hou X, Liu S, Wang M, Wiraja C, Huang W, Chan P, et al. Layer-by-Layer 3D Constructs of Fibroblasts in Hydrogel for Examining Transdermal Penetration Capability of Nanoparticles. Journal of Laboratory Automation. 2016: 2211068216655753.

92. Zhang YS, Arneri A, Bersini S, Shin S-R, Zhu K, Goli-Malekabadi Z, et al. Bioprinting 3D microfibrous scaffolds for engineering endothelialized myocardium and heart-on-a-chip. Biomaterials. 2016; 110: 45-59.

93. Ma X, Qu X, Zhu W, Li Y-S, Yuan S, Zhang H, et al. Deterministically patterned biomimetic human iPSC-derived hepatic model via rapid 3D bioprinting. Proceedings of the National Academy of Sciences. 2016; 113: 2206-11.

94. Bhise NS, Manoharan V, Massa S, Tamayol A, Ghaderi M, Miscuglio M, et al. A liver-on-a-chip platform with bioprinted hepatic spheroids. Biofabrication. 2016; 8: 014101.

95. Chang R, Emami K, Wu H, Sun W. Biofabrication of a three-dimensional liver micro-organ as an in vitro drug metabolism model. Biofabrication. 2010; 2: 045004.

96. Zhao Y, Yao R, Ouyang L, Ding H, Zhang T, Zhang K, et al. Three-dimensional printing of Hela cells for cervical tumor model in vitro. Biofabrication. 2014; 6: 035001.

97. Dai X, Ma C, Lan Q, Xu T. 3D bioprinted glioma stem cells for brain tumor model and applications of drug susceptibility. Biofabrication. 2016; 8: 045005.

98. Koike N, Fukumura D, Gralla O, Au P, Schechner JS, Jain RK. Tissue engineering: Creation of long-lasting blood vessels. Nature. 2004; 428: 138-9.

99. Bianco P, Cao X, Frenette PS, Mao JJ, Robey PG, Simmons PJ, et al. The meaning, the sense and the significance: translating the science of mesenchymal stem cells into medicine. Nature Medicine. 2013; 19: 35-42.

100. Huang X, Zhang F, Wang H, Niu G, Choi KY, Swierczewska M, et al. Mesenchymal stem cell-based cell engineering with multifunctional mesoporous silica nanoparticles for tumor delivery. Biomaterials. 2013; 34: 1772-80.

101. Zhang YS, Wang Y, Wang L, Wang Y, Cai X, Zhang C, et al. Labeling Human Mesenchymal Stem Cells with Gold Nanocages forin vitroand in vivoTracking by Two-Photon Microscopy and Photoacoustic Microscopy. Theranostics. 2013; 3: 532-43.

102. O'brien FJ. Biomaterials & scaffolds for tissue engineering. Materials today. 2011; 14: 88-95.

103. Seol Y-J, Park JY, Jeong W, Kim T-H, Kim S-Y, Cho D-W. Development of hybrid scaffolds using ceramic and hydrogel for articular cartilage tissue regeneration. Journal of Biomedical Materials Research Part A. 2015; 103: 1404-13.

104. Kim SH, Lee JH, Hyun H, Ashitate Y, Park G, Robichaud K, et al. Near-Infrared Fluorescence Imaging for Noninvasive Trafficking of Scaffold Degradation. Scientific Reports. 2013; 3: 1198.

105. Zhang Y, Rossi F, Papa S, Violatto MB, Bigini P, Sorbona M, et al. Non-invasive in vitro and in vivo monitoring of degradation of fluorescently labeled hyaluronan hydrogels for tissue engineering applications. Acta Biomaterialia. 2016; 30: 188-98.

106. Kim HJ, Lee S, Yun H-W, Yin XY, Kim SH, Choi BH, et al. In vivo degradation profile of porcine cartilage-derived extracellular matrix powder scaffolds using a non-invasive fluorescence imaging method. Journal of Biomaterials Science, Polymer Edition. 2016; 27: 177-90.

107. Huang S, Wang K, Wang S, Wang Y, Wang M. Highly Fluorescent Polycaprolactones with Tunable Light Emission Wavelengths across Visible to NIR Spectral Window. Advanced Materials Interfaces. 2016; 3: 1600259.

108. Sung KE, Beebe DJ. Microfluidic 3D models of cancer. Advanced Drug Delivery Reviews. 2014; 79–80: 68-78.

109. Ng WL, Wang S, Yeong WY, Naing MW. Skin Bioprinting: Impending Reality or Fantasy? Trends in Biotechnology. 2016; 34: 689-99.

110. Morgan MM, Johnson BP, Livingston MK, Schuler LA, Alarid ET, Sung KE, et al. Personalized in vitro cancer models to predict therapeutic response: Challenges and a framework for improvement. Pharmacology & Therapeutics. 2016; 165: 79-92.

111. Chung E, Nam SY, Ricles LM, Emelianov SY, Suggs LJ. Evaluation of gold nanotracers to track adipose-derived stem cells in a PEGylated fibrin gel for dermal tissue engineering applications. International Journal of Nanomedicine. 2013; 8: 325-36.

112. Blocki A, Beyer S, Dewavrin J-Y, Goralczyk A, Wang Y, Peh P, et al. Microcapsules engineered to support mesenchymal stem cell (MSC) survival and proliferation enable long-term retention of MSCs in infarcted myocardium. Biomaterials. 2015; 53: 12-24.

113. Han J, Kim B, Shin J-Y, Ryu S, Noh M, Woo J, et al. Iron Oxide Nanoparticle-Mediated Development of Cellular Gap Junction Crosstalk to Improve Mesenchymal Stem Cells' Therapeutic Efficacy for Myocardial Infarction. ACS Nano. 2015; 9: 2805-19.

114. Hua P, Wang YY, Liu LB, Liu JL, Liu JY, Yang YQ, et al. In vivo magnetic resonance imaging tracking of transplanted superparamagnetic iron oxide‐labeled bone marrow mesenchymal stem cells in rats with myocardial infarction. Molecular medicine reports. 2015; 11: 113-20.

115. Lee KG, Park KJ, Seok S, Shin S, Kim DH, Park JY, et al. 3D printed modules for integrated microfluidic devices. RSC Advances. 2014; 4: 32876-80.

116. Owens EA, Henary M, El Fakhri G, Choi HS. Tissue-Specific Near-Infrared Fluorescence Imaging. Accounts of Chemical Research. 2016; 49: 1731-40.

117. Bao K, Nasr KA, Hyun H, Lee JH, Gravier J, Gibbs SL, et al. Charge and hydrophobicity effects of NIR fluorophores on bone-specific imaging. Theranostics. 2015; 5: 609.

118. Hyun H, Owens EA, Wada H, Levitz A, Park G, Park MH, et al. Cartilage-Specific Near-Infrared Fluorophores for Biomedical Imaging. Angewandte Chemie International Edition. 2015; 54: 8648-52.

119. Hyun H, Park MH, Owens EA, Wada H, Henary M, Handgraaf HJM, et al. Structure-inherent targeting of near-infrared fluorophores for parathyroid and thyroid gland imaging. Nature Medicine. 2015; 21: 192-7.

120. Merceron TK, Burt M, Seol Y-J, Kang H-W, Lee SJ, Yoo JJ, et al. A 3D bioprinted complex structure for engineering the muscle–tendon unit. Biofabrication. 2015; 7: 035003.

121. Rimann M, Bono E, Annaheim H, Bleisch M, Graf-Hausner U. Standardized 3D bioprinting of soft tissue models with human primary cells. Journal of Laboratory Automation. 2016; 21: 496-509.

122. Nguyen D, Hägg DA, Forsman A, Ekholm J, Nimkingratana P, Brantsing C, et al. Cartilage Tissue Engineering by the 3D Bioprinting of iPS Cells in a Nanocellulose/Alginate Bioink. Scientific Reports. 2017; 7: 658.

123. Lee J-S, Kim BS, Seo D, Park JH, Cho D-W. Three-Dimensional Cell Printing of Large-Volume Tissues: Application to Ear Regeneration. Tissue Engineering Part C: Methods. 2017; 23: 136-45.

124. Kolesky DB, Truby RL, Gladman AS, Busbee TA, Homan KA, Lewis JA. 3D Bioprinting of Vascularized, Heterogeneous Cell-Laden Tissue Constructs. Advanced Materials. 2014; 26: 3124-30.

125. Liu Y, Chan JK, Teoh SH. Review of vascularised bone tissue-engineering strategies with a focus on co-culture systems. Journal of Tissue Engineering and Regenerative Medicine. 2015; 9: 85-105.

126. Baldwin J, Antille M, Bonda U, De-Juan-Pardo EM, Khosrotehrani K, Ivanovski S, et al. In vitro pre-vascularisation of tissue-engineered constructs A co-culture perspective. Vascular Cell. 2014; 6: 13.

127. Zhang C, Zhao Z, Rahim NAA, van Noort D, Yu H. Towards a human-on-chip: culturing multiple cell types on a chip with compartmentalized microenvironments. Lab on a Chip. 2009; 9: 3185-92.

128. Bhatia SN, Ingber DE. Microfluidic organs-on-chips. Nature Biotechnology. 2014; 32: 760-72.

129. Zhang X, Xu B, Puperi DS, Yonezawa AL, Wu Y, Tseng H, et al. Integrating valve-inspired design features into poly (ethylene glycol) hydrogel scaffolds for heart valve tissue engineering. Acta Biomaterialia. 2015; 14: 11-21.

130. Sridhar BV, Brock JL, Silver JS, Leight JL, Randolph MA, Anseth KS. Development of a cellularly degradable PEG hydrogel to promote articular cartilage extracellular matrix deposition. Advanced Healthcare Materials. 2015; 4: 702-13.

131. Kim BS, Jang J, Chae S, Gao G, Kong J-S, Ahn M, et al. Three-dimensional bioprinting of cell-laden constructs with polycaprolactone protective layers for using various thermoplastic polymers. Biofabrication. 2016; 8: 035013.